Universidade do Minho
Escola de Engenharia

Ana Catarina Cardoso Gil

Decoding human motion intentions from brain signals

October , 2022

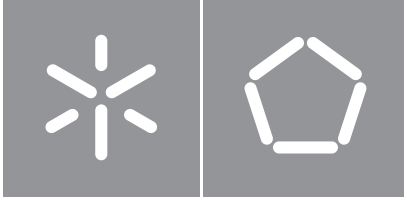

Universidade do Minho
Escola de Engenharia

Ana Catarina Cardoso Gil

Decoding human motion intentions from brain signals

Master's Dissertation
Integrated Master's in Informatics Engineering

Work supervised by
Professora Doutora Cristina P. Santos
Doutora Joana Figueiredo

October , 2022

STATEMENT OF INTEGRITY

I hereby declare having conducted this academic work with integrity. I confirm that I have not used plagiarism or any form of undue use of information or falsification of results along the process leading to its elaboration.

I further declare that I have fully acknowledged the Code of Ethical Conduct of the Universidade do Minho.

_____, _____

(Location) (Date)

_____

(Ana Catarina Cardoso Gil)

Acknowledgements

I would like to thank my supervisors, Dra. Cristina P. Santos and Dra. Joana Figueiredo, as well as Simão Carvalho, for their guidance throughout this project.

I also want to express my gratitude to my parents, who have been my biggest supporters in life and have helped me both financially and emotionally.

Abstract

Gait function can be affected by neurological disorders such as spinal cord injury (SCI), stroke, or traumatic brain injury (TBI). These limitations have significant negative effects on the affected people's independence and quality of life. Brain-computer interfaces (BCIs) have the potencial to create solutions that may overcome irreversible disabilities. Several studies in recent years have shown that electroencephalographic (EEG) signals can be used to develop BCIs for the rehabilitation of human limbs through lower-limbs robotic devices and exoskeletons. Therefore, their effectiveness and safety depend on how successfully they can detect and react to movement.

This dissertation aims at developing and validating an EEG-based motor intent decoding framework to accurately classify human intent regarding five daily performed locomotor tasks. This framework will contribute on the developing of BCI to recover the mobility of neurologically impaired subjects. For this, a provided multi-channel dataset will be used.

The implementation of this solution was divided into two phases. The first is about how signals are processed to obtain the features that best characterize each of the locomotion modes under analysis. As a result, three distinct studies that differ in the number of channels used were created. Through the application of the ICA method, it has been determined that the more channels are used in a study, the more likely it is that these channels may be corrupted, affecting the ICA method's effectiveness.

The second section discusses the classification methodology. Three different Deep Learning algorithms, CNN, LSTM, and their combination, C-LSTM, were studied here. Additionally, three different features used as the input for the models were compared for each of them and for each of the studies.

The features that were selected showed a higher impact on the results than the actual classification algorithm, with ERPs being the features that produced the best results. On the other hand, across classifiers, all three provided high performance, demonstrating reduced differences between them. The study with higher accuracy as the study 3 with the most reliable channel selection.

Keywords: brain-computer interface (BCI); electroencephalogram (EEG); motor intention decoding; Signal processing

Resumo

O movimento humano da marcha pode ser afetado por distúrbios neurológicos, tais como lesão na medula espinhal, acidente vascular cerebral (AVC), ou traumatismo craniano. Estas limitações têm efeitos negativos significativos tanto a nível de independência, como na qualidade de vida das pessoas afetadas. Interfaces cérebro-computador (BCIs) mostram ter potencial para fornecer soluções para o tratamento de distúrbios cerebrais. Nos últimos anos, vários estudos mostraram que sinais eletroencefalográficos (EEG) podem ser usados no desenvolvimento de BCIs para a reabilitação de membros humanos através de equipamentos robóticos de membros inferiores e exoesqueletos. A sua eficiência e segurança dependem do sucesso com que conseguem detetar e reagir ao movimento.

Esta dissertação tem como objetivo desenvolver e validar um framework de decodificação de intenção motora baseada em EEG para classificar com precisão a intenção humana segundo cinco tipos de locomoção presentes no dia-a-dia. Este framework irá contribuir para o desenvolvimento de um BCI com a finalidade de recuperar a mobilidade de sujeitos com deficiência neurológica. Para isso, será utilizado um dataset multicanal já existente.

A implementação desta solução foi dividida em duas fases. A primeira refere-se ao processamento dos sinais para obter as features que melhor identificam cada um dos modos de locomoção em análise. Como resultado, foram criados três estudos distintos que diferem no número de canais utilizados. Através da aplicação do método ICA, foi concluido que quanto mais canais forem utilizados num estudo, maior é a probabilidade de existirem canais corrompidos, afectando a eficácia dos resultados.

A segunda secção discute a metodologia de classificação. Três diferentes algoritmos de Deep Learning, CNN, LSTM, e a sua combinação, C-LSTM, foram estudados. Além disso, foram comparadas três features diferentes utilizadas como input para cada um dos modelos e para cada um dos estudos.

As Features que foram seleccionadas mostraram um maior impacto nos resultados do que o próprio algoritmo de classificação, sendo os ERPs as features que obtiveram os melhores resultados. Por outro lado, todos os modelos apresentaram um bom desempenho, não havendo diferenças significativas entre eles. O estudo que obteve maior precisão foi o estudo 3.

Palavras-chave: interface cérebro-computador (ICC); eletroencefalografia (EEG); decodificação de intenção motora; processamento do sinal

Contents

List of Figures

List of Tables

Acronyms

ASR Artifact Subspace Reconstruction

AUC Area Under the Curve

BA Balanced Accuracy

BCI Brain Computer Interface

BP Bereitschafts Potential

BP Band Power

CAR Common Average Reference

CNN Convolutional Neural Network

CSP Common Spatial Pattern

CV Channel Variance

DL Deep Learning

DWT Discrete Wavelet Transform

EEG Electroencephalography

EMG Electromyography

ERD Event-Related Desynchronization

ERP Event Related Potentials

ERS event-related Synchronization

ERSP Event-related Spectral Perturbation

FES Functional Electrical Stimulation

FFT Fast Fourier Transform

FIR Finite Impulse Response

GA Genetic Algorithm

GMM Gaussian Mixture Modelling

ICA Independent Component Analysis

IIR Infinite Impulse Response

KNN K-Nearest Neighbors

LDA Linear Discriminant Analysis

LFDA Local Fisher's discriminant analysis

LSTM Long short-term memory

MA Motor Attempt

MCC Matthews Correlation Coefficient

ME Motor Execution

MI Motor Imagery

ML Machine learning

MMP Movement-Monitoring Potential

MP Motor Potential

MRCP Movement-Related Cortical Potential

PCA Principal Component Analysis

PSD Power Spectral Density

QDA Quadratic Discriminant Analysis

RNN Recurrent Neural Network

RP Readiness Potential

SCI Spinal Cord Injury

SL Surface Laplacian

SMA Supplementary Motor Area

SMR Sensory Motor Rhythms

SNR Signal-to-Noise Ratio

SVM Support Vector Machine

TDP Time Domain Parameters

Chapter 1

Introduction

This dissertation was developed in the Master in Informatics Engineering of University of Minho. The Master's thesis will be carried out in Biomedical Robotic Devices Lab included in the Center for Micro-ElectroMechanical Systems (CMEMS), a research center from the University of Minho. In this chapter will be presented the motivation behind this dissertation, explaining the existing problems in this society and solutions available for trying to answer the existing needs. The dissertation's objective and goals will also be presented. In the following section, the state-of-the-art will be discussed. Finally, a list containing each of the dissertation's objectives as well as its schedule will be provided.

1.1 Context and motivation

Injured subjects such as stroke survivors and patients with spinal cord injury may exhibit loss of motor control and muscle weakness [1]. Furthermore, amputation of a lower limb due to accident or diabetes is another cause that results in decreased mobility. Robotic assistive devices such as prostheses, exoskeletons, and functional electrical stimulation have potentiated the improvement and restoration of impaired locomotion. Despite this, to achieve a natural and effective restoration, the subject must fully and voluntarily control the devices [2].

Sensorimotor rehabilitation is an important part of post-brain injury treatment, with the goal of recovering motor control and increasing independence and quality of life [3]. For this purpose, Brain Computer Interface (BCI) has been used to enable humans to interact and control external devices using electrical signals measured from their brain activity through EEG [4]. A lower extremity prosthesis controlled by a BCI might be a truly innovative solution. An implanted Functional Electrical Stimulation (FES) device and an invasive brain signal acquisition system can be used to establish a reliable BCI prosthetic. However, for

reasons of safety, noninvasive methods must be used to test the viability of brain-controlled locomotion first [5].

The capacity to predict human movement intent is critical for successful gait rehabilitation [6]. EEG signals can act as a real-time projection of the brain's motor activity during gait. EEG-based gait studies hold significant potential in achieving early prediction of the human motion intention than kinematics and electromyography [6]. Current directions focused on developing artificial intelligence tools fed by BCI's data to decode human motor intention and timely adjust robotic assistance according to the human intent. Thus, researchers can readily adopt this setup for more effective rehabilitation of motor-impaired persons providing them with necessary motor capabilities [6].

1.2 Problem statement

EEG motor detection upper-limb studies are extensively researched, but fewer have focused into lower-limb movement intention decoding [7]. Those that studied on the lower limbs are mostly done with Motor Imagery (MI).

Previous studies using machine learning models successfully classified binary-class states, mostly gait and stand states. Only sitting and standing intents were used in research that attempted to decode more complex movements [8]. However, studies to detect multi-class movements are still limited.

Although conventional BCI systems have progressed a lot in recent decades, EEG classification still remains a major challenge for researchers, due to biological and environmental artifacts in EEG, a low Signal-to-Noise Ratio (SNR), and dependency on human skill for extracting meaningful features [9]. Deep Learning (DL) architectures have been used to extract significant information from signals that was previously impossible to get using traditional methods, and has demonstrated progress in solving this previous difficulties. Additionally, there isn't a processing and classification framework for EEG that could be used as a guide. Therefore, more research is required to identify and establish well-defined procedures.

1.3 Goal and objectives

The main goal of this work is to develop and validate a DL framework based on EEG signals to decode a set of locomotion modes performed daily, namely: level-ground walking, ascending/descending stairs and ramps. In order to reach this goal, a public dataset with EEG signals from healthy locomotion was used. Further, this work studies the processing methods required to remove noise and artifacts from EEG data and the EEG feature that best represent each locomotion mode. This dissertation will also benchmark different DL algorithms towards the identification of the most accurate classification model.

In order to reach this ultimate goal, it is necessary to achieve the following objectives:

1. Objective 1: To review related studies on EEG-based locomotion mode classification. First, to review BCI system and current applications. Second, to identify commonly applied processing methods to removal artifacts from EEG signals. The reviewed information will support the developments in Chapter 3. Third, to review the used classification algorithms and the decoded locomotion tasks from EEG signals. This review will serve as a base for the design and development of DL framework proposed in Chapter 4. Chapter 2 presents these surveys.

2. Objective 2: To process EEG dataset to remove noise and artifacts by studying the best processing algorithms and parameters. Chapter 3 addresses this objective.

3. Objective 3: To identify the best EEG channel configuration, studying the channels commonly used in the literature to monitor the sensorimotor cortex and the channels with higher signal quality. Chapter 3 studies the EEG channels and the best ones are identified based on the results presented in Chapter 4.

4. Objective 4: To compute the EEG features in the frequency domain from the selected channel configuration and identify the ones that best represent each locomotion mode. Chapter 3 computes the EEG features, and the best ones are identified based on the results presented in Chapter 4.

5. Objective 5: To develop and validate a locomotion mode decoding framework based on the computed EEG features. This objective enables to identify the best classifier from a benchmarking between three different DL algorithms. Chapter 4 addresses this objective.

1.4 Research Questions

As previously stated, the goal of this thesis is to develop an EEG-based decoder. However, since no accurate or pre-defined methodology for it development has been identified in the literature, the implementation of this framework will also help to address certain questions.

The following research questions (RQs) are proposed and expected to be answered:

- RQ1: Which are the best removal artifacts algorithms to yield useful EEG data from human locomotion?
- RQ2: What is the number of channels that yields the highest decoding performance?
- RQ3: What is the EEG feature in the frequency domain that best represents locomotion modes?
- RQ4: What is the best DL classifier to decode locomotion modes from EEG data?

Chapter 2

State of the Art

2.1 Motor-based BCI

2.1.1 BCI systems

A brain-computer interface (BCI) is an artificial intelligence system that collects, analyzes and converts brain signals into commands that are sent to an output device to perform a desired action [10]. A BCI is a technology that develops a new way of communicating with machines by utilizing just the brain. Unlike other interfaces, BCI does not need to involve real movement, and so may be the only way to communicate for people with severe motor limitations.

Typically, a BCI system is composed by six mechanisms: brain signal acquisition, pre-processing, feature extraction, classification, translation into a command and feedback [11], as shown in Figure 1.

1. Brain Signal Acquisition: BCIs had two different techniques to measure brain signals: non-invasive, which is based on signals collected from electrodes inserted on the scalp (outside the head), and invasive, which is based on signals recorded from electrodes implanted over the cerebral cortex (requires surgery) [12]. Normally, invasive techniques provide higher signal quality when compared to non-invasive approaches. Examples of invasive methods are electrocorticography (ECoG) and single-neuron recordings. Non-invasive methods are Electroencephalogram (EEG), Magnetoencephalogram (MEG), Positron Emission Tomography (PET), Functional Magnetic Resonance Imaging (fMRI) and Near-Infrared Spectroscopy(NIRs) [13].

2. Pre-processing: After signal acquisition, pre-processing is used to reduce any noise or artifacts that were captured when obtaining the signals of the devices. The undesired signals can be: some

inference, whenever an electronic equipment is attached; Electromyography (EMG) signals that are produced by some muscular action; ocular artifact caused by eye movement or blinking. Unwanted noises in the EEG recording can result in erroneous conclusions and affect the interpretation of the EEG readings. As a result, several filters are utilized to reduce noise from signals. In general, pre-processing is the technique of transforming raw data into a format that is more suited for future analysis and understandable to the user [14].

3. Feature Engineering: The creation, transformation, extraction, and selection of features, also known as variables, are all procedures of feature engineering. The goal of feature engineering is to identify the smallest and most informative feature set (distinct patterns) in order to improve the classifier's performance [15]. This stage is crucial for extracting meaningful characteristics from the large number of signals obtained [16].

4. Classification: This stage is also known as "feature translation". The role of the classification component is to translate the features provided by the feature extractor to a brain patterns category.

5. Translation into a command/application: Based on the identification of the mental state, a command is connected with it in order to control a the application, such as a computer or a robot.

6. Feedback: This stage gives the user feedback, typically if it is right or wrong, on the mental state that has been identified. The ultimate goal is to improve the performance of the users.

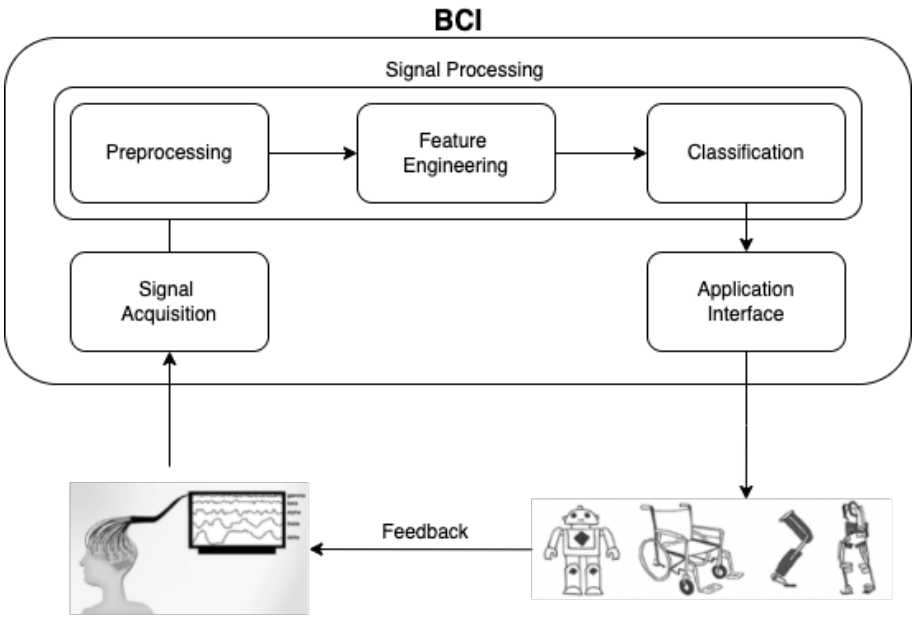

Figure 1: A general architecture of a BCI system. Adapted from: [4, 17]

To avoid the risks of surgery, many BCI researchers opt for a non-invasive methods. Due to its benefits, which include greater temporal resolution, lower costs, mobility, and non-invasiveness, EEG has been the most extensively used approach for brain signal analysis and classification [18].

An EEG is a noninvasive recording of brain activity. It is performed by attaching special sensors, called electrodes, to the head and connecting them to a computer that records the brain's electrical activity, which is displayed as a series of wavy lines. Figure 2 depicts an EGG recording session while walking on a treadmill. A conventional EEG signal has an amplitude of approximately 10 µV to 100 µV and a frequency of 1 Hz to 100 Hz. EEG signals are non-Gaussian, non-stationary, and non-linear [19].

The connection between the scalp cap and the computer can be made either wired or wireless. Wired EEG connections are more robust and can typically transfer more data in less time, but they lack the mobility that wireless connections provide. One of the major disadvantages of wireless EEG devices is that they may lose connectivity during data collection and hence fail to record the data. These devices may have one or more additional channels for recording physiological signals such as Electrocardiogram (ECG), Electrooculography (EOG), Photoplethysmogram (PPG), and Electromyography (EMG) [20].

Figure 2: EEG recording during treadmill walking in a healthy subject with anAg/AgCl 128-scalp-electrode cap (Waveguard®, ANT Neuro, Enschede, The Netherlands) [21].

The International Federation of Societies for Electroencephalography designed a 10–20 electrode placement system to specify electrode locations. The 10–20 system is based on the relationship between an electrode location and the underlying cerebral cortex region [19]. Therefore, as shown in the Figure 3, each electrode location is labeled with a letter that identifies the part of the brain it is reading from: pre-frontal (Fp), frontal (F), temporal (T), parietal (P), occipital (O), and central (C). The right side is represented

by even numbers (2,4,6,8), while the left side is represented by odd numbers (1,3,5,7). The z stands for a midline electrodes. The locations A1 and A2 act as a contralateral reference.

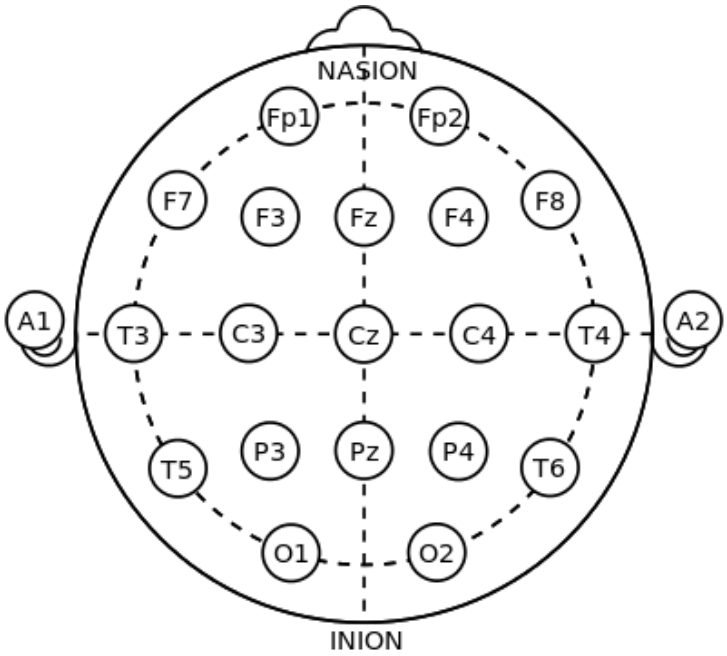

Figure 3: Electrode locations of International 10-20 system for EEG recording [22]

As the usage of EEG signals increased over the years, the development and innovation of equipment to acquire them did too. Table 1 ranks each EEG hardware based on the number of publications it has been linked to, with the most used being NeuroScan, Brain Products, BioSemi . For human motor decoding, LiveAmp and ActiCAP by Brain Products GmbH [8, 23–26] and Nautilus by g.tec [27–29] are the most used EEG devices in the literature.

Table 1: Top 8 EEG Hardware Companies [30]

EEG Hardware Companies	No. Channels	No. Publications
NeuroScan	Up to 256	12300
Brain Products	8–64	6690
BioSemi	Up to 144	5750
EGI	Up to 128	5000
Emotiv	Up to 32	3990
NeuroSky	2	2290
Advanced Brain Monitoring	Up to 24	790
g.tec	8, 16, 32, 64	430

EEG waves are generally classified by their frequency, amplitude, shape, and the locations on the scalp where they are recorded. The most familiar classification uses EEG waveform frequency, which divides the signals into five main ranges between 0 and 100 Hz: delta, theta, alpha, beta and gama, as it is shown in table 2. Beta waves are most frequently related to actions and behavior since signals in this band are

associated with the senses of touch, hearing, smell, and taste. Beta waves occur in a conscious state and have a frequency range of 13 Hz to 30 Hz, whereas alpha waves (mu-rhythm) have a frequency range of 8 Hz to 13 Hz and are related to motor cortex functions [31].

Table 2: EEG frequency bands and related mental states.

Wave	Frequency Range (Hz)	Amplitude Range (μV)	Brain State
Delta	0 - 4	20-100	Deep Sleep
Theta	4 - 8	10	Deep Meditation
Alpha	8 - 13	2-100	Eyes closed, awake
Beta	13 - 30	5-10	Eyes opened, thinking
Gama	30 - 100	-	Cognition, information processing

2.1.2 Motor-related EEG

Recently, a significant number of studies have investigated brain activity during human movement, with a particular focus on the use of EEG. Previous research has discovered that brain activity increases during walking or the preparation for walking, and the sensorimotor area is significantly activated during isolated leg or foot motions [32].

The cortical sensorimotor rhythms may be elicited in the brain during the execution/attempt or imagination of motor activities. Motor Execution (ME) is a term that refers to a certain movement that is actually performed. Motor Attempt (MA) is comparable to ME. However, it is typically used when ME is not a possibility, such as in the case of paralysis following a stroke or Spinal Cord Injury (SCI). MI is defined as the internal reactivation of any first-person motor performance without an overt motor output. ME/MA as well as MI paradigms have been used in the design of BCIs. Although the majority believe there is no big difference, some researches reported that motor cortical excitability is significantly lower during MI than it is during ME, and ME has demonstrated better performance. [33–35]. Nonetheless, MI motor-based BCI's are the most used in literature [36].

The cerebral cortex is the most significant structure in EEG measurements [37]. Because different lobes of the cerebral cortex are responsible for processing different kinds of activity, the decision of where to place the electrodes is important. Delval et al. [38] applied three different methods, sLORETA, dSPM, and wMNE, for source localization on EEG signal (4–30 Hz) during gait initiation. All three methods showed sources in premotor cortex, supplementary motor area, and primary motor cortex. Both sLORETA and dSPM showed sources on left temporal lobe too.

The primary motor cortex, the premotor cortex and the Supplementary Motor Area (SMA) are three areas from motor cortex related to human motion.. The motor cortex is a part of the cerebral cortex, located in the frontal lobe, that is known to be responsible for voluntary movement execution, planning, and control [39]. Primary motor cortex contains upper motor neurons, which represent the first primary output of the motor system. In general, primary motor cortex encodes the parameters that define individual

movements such as force, direction and speed. The premotor cortex transmits axons to the primary motor cortex as well as directly to the spinal cord. SMA is responsible for coordinating bilateral motions and programming more complex movement sequences. Therefore, it appears that the premotor cortex is involved in motor plans for voluntary movements based on visual stimulation while the SMA select movements based on remembered sequences of movements. Thus, primary motor cortex is responsible for their execution [40].

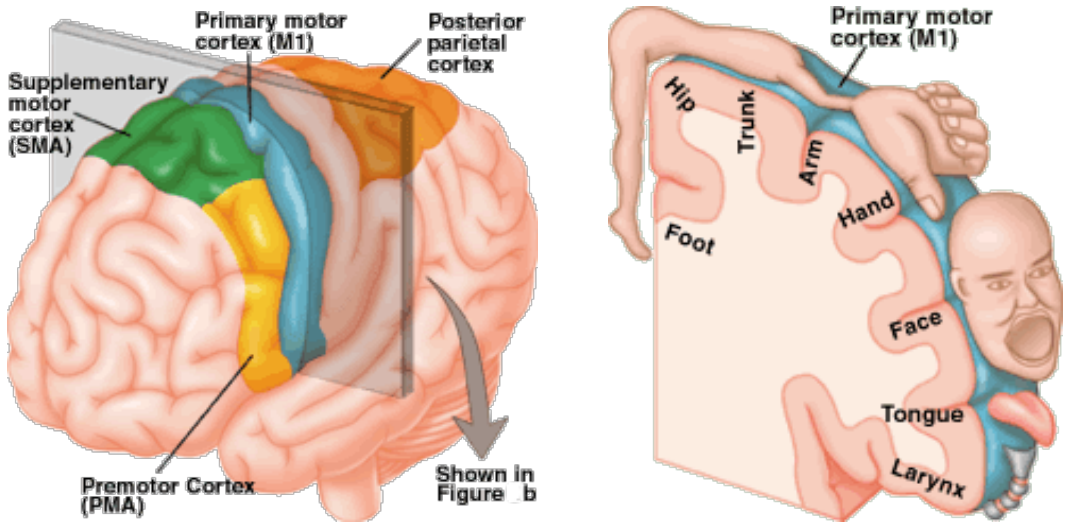

(a) Principal cortical domains of the motor system.

(b) The motor homunculus in primary motor cortex.

Figure 4: The brain anatomy of movement [41]

BCIs have made a difference in a range of fields. They work in the areas of medicine, neurorehabilitation, and smart environments, as well as neuromarketing and advertising, education and self-regulation, gaming and entertainment, and security and authentication. Helping individuals with disabilities or motor activity impairments is one of the most important BCI applications. Motor-based BCIs are currently being researched for two clinical applications [42]:

- Assistive technologies that aim to recover lost functions, such as communication or movements in paralysis, using robotic actuators and/or functional electrical stimulation systems.
- Rehabilitation technologies, often known as neurofeedback or rehabilitative BCIs, that attempt to promote neuroplasticity by manipulating or self-regulating neurophysiological activity in order to aid motor recovery.

As a result, the most outstanding researches include: controlling an electric wheelchair[43–46], controlling a prosthetic hand or arm[47–49], detecting a patient's attempt to move their body [50, 51].

2.2 EEG-based locomotion intention decoding

It is essential for an effective assistive system to detect the movement intention as early as possible in order to provide the system enough time to adjust to the individual's needs. When it comes to movement intention recognition, there are two primary neural features that have been observed in the brain's preparation for voluntary movements. Those are event-related patterns in the time domain named Movement-Related Cortical Potential (MRCP) and patterns in the frequency domain named Sensory Motor Rhythms (SMR).

The MRCP corresponds to self-paced movement, and it is defined by a slow decrease in EEG amplitude over the primary motor cortex within at least 2s preceding movement onset [6]. It's especially useful in BCI applications where the time between the movement intention and the system's feedback is critical for inducing plasticity. As shown in figure 5, the MRCP is formed by three events: Readiness Potential (RP) or Bereitschafts Potential (BP), Motor Potential (MP), and Movement-Monitoring Potential (MMP), which are assumed to reflect movement planning/preparation, execution, and control, respectively [52].

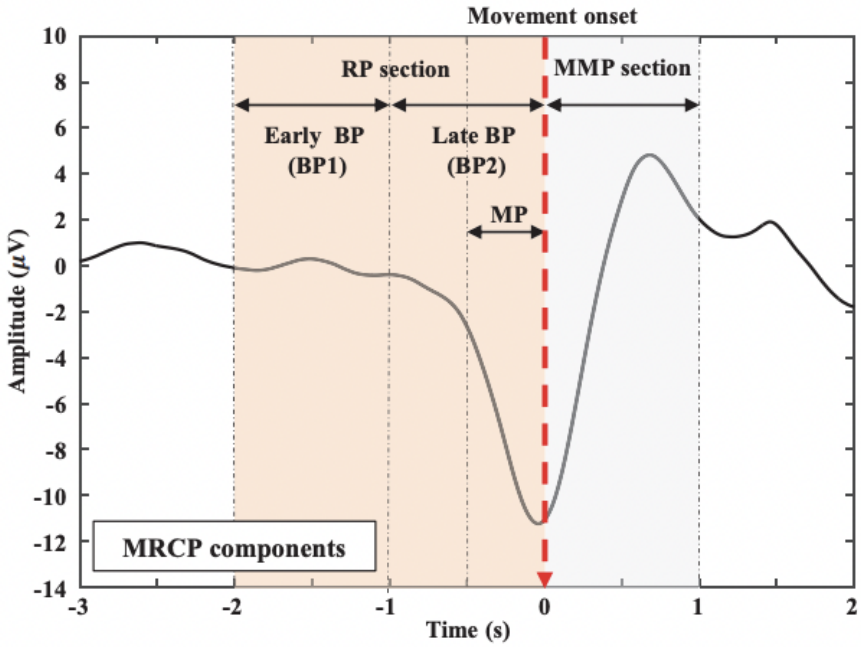

Figure 5: MRCP amplitude fluctuation at the Cz electrode [53]

SMRs, on the other hand, have been used to decode movement intent as an alternative to MRCPs. The most frequent SMRs are Event-Related Desynchronization (ERD) and event-related Synchronization (ERS) which refer to the decrease and increase, respectively, of power in EEG frequency bands. As seen in Figure 6, the ERS is detected a few seconds after the movement onset, making it less common in studies for intent detection. As a result, much of the SMR-based intent detection literature relies solely on the power decrease, or ERD. ERD is characterized as a 0.5–2s decrease in spectral power before movement

onset [7].

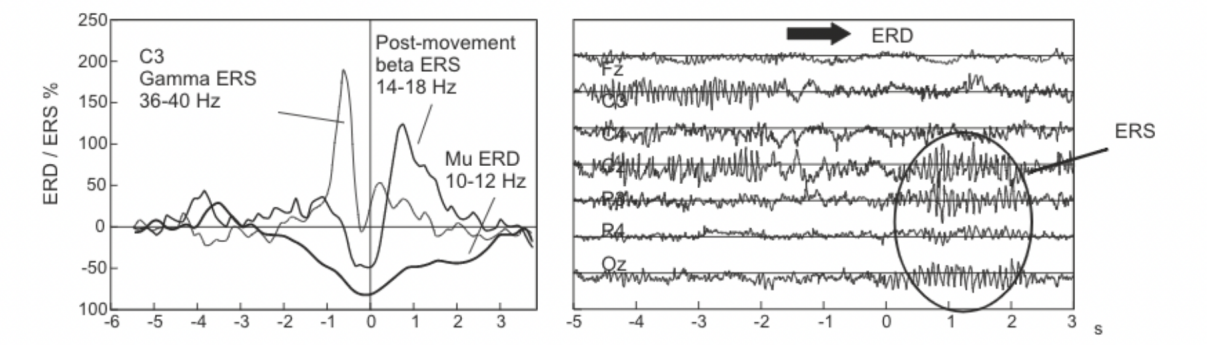

Figure 6: Left panel: Superimposed band power time courses for 10–12 Hz, 14–18 Hz, and 36–40 Hz frequency bands; Right panel: Right finger movement EEG records [54].

In Seeland et al. [55] MRCP and ERD/ERS classification performance of pre-movement components at different time windows and electrode groups were compared. They found spatiotemporal variations in the performances of ERD/ERS and MRCP, indicating that ERD/ERS is more effective far away from the movement onset, while MRCP performs better towards the movement initiation. At time points of 0.04s and 0.0s, respectively, optimal classification accuracies for ERD/ERS and MRCP were found, with MRCP classification outperforming ERD/ERS detection. When all 68 channels were used during training, overall classification performance for both brain signals improved, mainly for MRCP (ERD/ERS: 0.72±0.012 Balanced Accuracy (BA), MRCP: 0.8±0.012 BA). Figure 7 shows the evolution of performance for the MRCP and ERD/ERS classifications, respectively.

Liu et al. [7] employed a BCI to decode the intention of self-paced lower-limb movement. The study was based on four factors: movement type (dorsiflexion or plantar flexion), limb side, processing method (MRCP or SMR), and frequency band. Plantar flexion with the left leg provided the greatest results using time-series analysis on the MRCP band [0.1-1] Hz. The average Area Under the Curve (AUC) for the MRCP-based and SMR-based methods in classification was 91.0 ± 3.5% and 68.2 ± 4.6%, respectively.

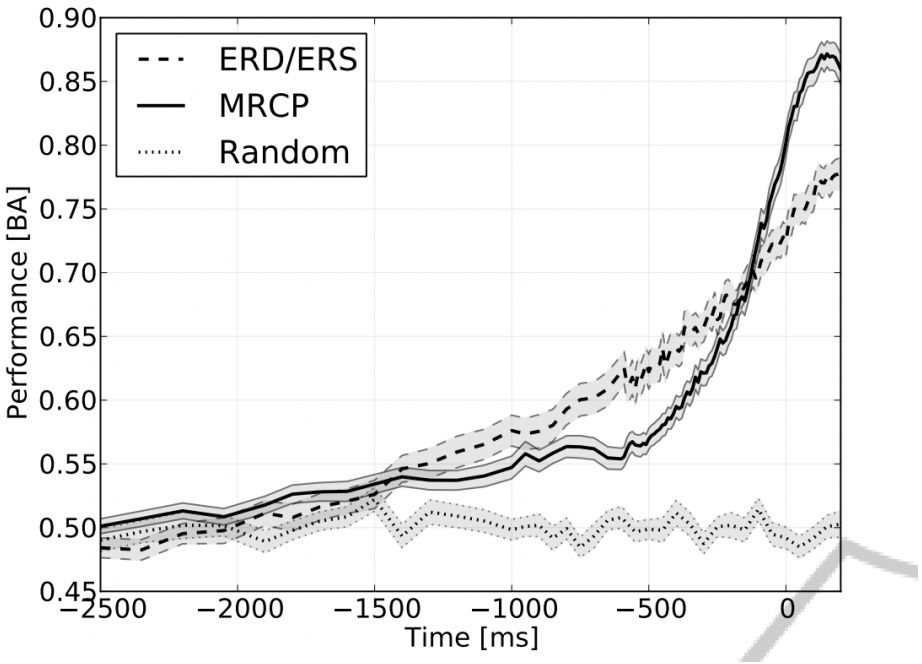

Figure 7: Averaged classification performance across splits and subjects over time for classifiers based on ERD/ERS and MRCP [55].

ERD/ERS and MRCP are sometimes used together or individually. In the literature, however, there is no agreement on whether ERD/ERS and MRCP should be combined or not. Some authors propose a hybrid approach [56–58]. Others, on the other hand, believe that extracting features from both patterns does not provide benefits [59].

2.2.1 Signal Preprocessing

There are several reasons why EEG data must be preprocessed. To begin with, the signals picked up from the scalp are not always a precise representation of the original brain signal, as spatial information gets lost. Second, EEG data contains a lot of noise, which might hide weaker EEG signals [18]. Because EEG preprocessing is still a developing field, there is no globally accepted pipeline, which means that researchers have considerable freedom in deciding how to process the raw data [60]. As a result, multiple methods for removing undesired noise and artifacts from EEG data have been proposed.

The two main types of artifacts in EEG signals are [61]:

(i) physiological/biological, like cardiovascular, pulse, respiratory, sweat, glossokinetic, eye movement, and muscle and movement artifacts, and

(ii) nonphysiological, caused by electrical phenomena or devices in the recording environment.

In particular for BCI, EEG signals are typically filtered in the time domain and spatial domain before features are extracted from the resulting signals.

Filtering in the Time Domain Almost all researches employ the process of filtering in time domain for decreasing noise. The most popular filters are low, high, and band-pass. These kinds of filters allow frequencies that are bellow, above, or between defined values, respectively.

Filters can be designed to have a Finite Impulse Response (FIR) or Infinite Impulse Response (IIR). An impulse response is simply how the filter handles a unit impulse signal in the time domain. Normally a Fourier transform is used to analyze its frequency response [62]. Almost all studies recommend the use of FIR filters. They are easier to control, are always stable, have a well-defined passband, can be corrected to zero-phase without additional computations, and can be converted to minimum-phase. IIR filters are usually considered to be more computationally efficient, but they are only recommended when high throughput and sharp cutoffs are required, usually when it is online [63].

Khatter et al. (2019) [64] focuses on removing random noise from EEG signals by using digital IIR filter and multiple FIR window filters (Hanning, Hamming, Kaiser, Blackman) of various orders to perform a low-pass filter. The mean square error, mean absolute error, signal to noise ratio, peak signal to noise ratio, and cross-correlation were used in their performance analysis. The results show that the FIR filter based on the Kaiser Window with an order of 4 to 6 outperforms in denoising different EEG signals than the IIR and other FIR filters.

Similar to this, Veer et al. (2016) [65] performance analysis of FIR filter based on various windows and IIR filters of 100th order for noise reduction. The fast Fourier transform and signal-to-noise ratio were used to analyze performance. Once again, Kaiser window-based FIR filters were shown to be better at eliminating power-line noise from EEG signals. This filtering is used to select the frequency ranges of interest in the EEG by removing or extracting parts of a signal. In ERD, the power decrease is most commonly observed in the alpha band over the motor and somatosensory cortex, also known as the mu-rhythm bands [7]. McFarland et al. [66], Tam et al. [67] and Yuan and He [68] have concluded when a subject performs actual or even imagined movement, the signal power in the 8–13 Hz range is decreased. In the lower beta band, similar observations can also be seen. In Wang et al [69] a BCI-based lower limb exoskeleton control system based on MI was developed. To eliminate effects such as eye blink (4 HZ) and power frequency interference (50 HZ), a bandpass IIR filter was adopted with the frequency set to 5-35 Hz and the order set to 8.

However, when the research is aimed at MRCPs, signals are filtered in a lower frequency range, typically between 0–5 Hz [70]. As a result, most approaches focus exclusively on the delta band [70–72].

Filtering in the Spatial Domain The most used spatial filters are algorithms like (Common Average Reference (CAR)) [56, 73–75], Surface Laplacian (SL) [56], Artifact Subspace Reconstruction (ASR) [8, 23, 24, 29, 71, 76], Independent Component Analysis (ICA) [23] and H^{∞} adaptive filtering [23, 76]. ICA, like Principal Component Analysis (PCA), determines channel weighting from data, but CAR and SL linearly combine channels to give a set of weights that is independent of the underlying data [52]. The majority of

research employ several spatial filters.

According to Bulea et al. [8], ASR is successful in removing high amplitude artifacts from EEG data and it does not modify EEG during pre-movement periods. Several articles highlight the benefits of combining ASR and ICA methods [6]. Pion-Tonachini et al. [77] propose combining online ASR and online recursive ICA to remove artifacts with large amplitudes. The pipeline was performed in the presence of six distinct EEG artifacts, including movement and muscle artifacts, as well as cued blinks. The most of the artifact-induced signal features were found to be removed. It was also compared with and without an initial application of ASR, and it was revealed that the presence of ASR stabilized the ORICA decomposition, which is desired for removing eye movement-related artifacts from data. Chang et al. [78] also performed a combination between ASR and ICA for automatic artifact component removal. The results showed that ASR removes more eye and muscle components than brain components, and while some eye and muscle components remain after ASR cleaning, their temporal activity power is decreased. Also, ASR cleaning increased the quality of ICA decomposition.

In McFarland et al. [79], a study was conducted to compare alternative spatial filtering methods. EEG data was collected from 64 channel while subjects were moving the cursor to targets at the top or bottom edge of a video screen. It were analyzed offline by four different spatial filters, namely a standard ear-reference, CAR, a small Laplacian and a large Laplacian. The CAR and large Laplacian methods proved most able to distinguish between top and bottom targets. The CAR and Laplacian methods outperform the ear reference method, owing to the fact that they are high-pass spatial filters that enhance focal activity from local sources (e.g. the mu rhythm and closely related beta activity) while reducing widely distributed activity, including that from distant sources (e.g. EMG, eye movements and blinks).

2.2.2 Feature Engineering

Features are characteristics that are extracted from signals using a set of methods. These characteristics are the variables that are used as input to the classification algorithms. The main principle behind feature extraction is to reduce high-dimensional input data into a smaller representation set of features that contains the relevant information required for classification.

Feature engineering in machine learning includes four processes: feature creation, feature transformation, feature extraction, and feature Selection.

Feature creation is creating the most useful variables to use in a predictive model. This could include adding and removing some features. Usually, this is a subjective process that needs human interaction. A function that changes features from one representation to another is known as feature transformation. The idea is to plot and visualize data so that if anything doesn't add up with the new features, we may minimize the amount of features utilized, speed up training, or improve the accuracy of a model [80].

According to numerous researchers, selecting a good feature extraction method has a greater influence

on final performance than selecting a good classifier [81]. Feature extraction is an automated feature engineering method that generates new variables from raw data. The primary goal of this stage is to reduce the amount of data in order to make it easier for the model to use and manage.

EEG signals are time-domain signals and are non-stationary in nature. They can be represented in different ways. The most common types of features used to represent them are in time domain, frequency domain or time-frequency domain. The time domain features of EEG signals are used because they show an increase in amplitude, regularity, and synchronicity. Synchronicity is a metric that shows how similar signals are to one another. Frequency domain features such as energy, power, mean, and variability are amplitude related. Regularity are tested with variance and coefficient of variation. Total variation similarly synchronicity is evaluated with cross correlation and phase locking [82]. The most frequent spectral method is Power Spectral Density (PSD), because the power spectrum provides the signal's 'frequency content' or the distribution of signal power over frequency [83].

While EEG signals may be represented in a variety of ways, frequency band power features and time point features are the two most popular types of features used to describe EEG data [84]. Both benefit from being extracted after spatial filtering [85, 86]. Värbu [87] accomplished a systematic literature review on EEG-based BCI Applications, analyzing the most used feature extraction methods in research, and, as shown in the table 3, PSD, glsFFT and Common Spatial Pattern (CSP) are clearly the most often utilized techniques. In fact, the Fast Fourier Transform (FFT) and PSD methods are directly related, as FFT is commonly used in EEG to estimate PSD) [88]. PSD stands for spectral energy distribution per unit frequency.

Table 3: Feature extraction methods used in researches [87]

Feature Extraction	Number of researches
Power spectral density	23
Fourier transform	20
Common spatial pattern	18
Wavelet transform	8
Fractal dimension	7
Independent component analysis	7
Principal component analysis	7

In Bhattacharyya et al [82] study, the aim of the study is to compare the performance of Linear Discriminant Analysis (LDA), Quadratic Discriminant Analysis (QDA) and K-Nearest Neighbors (KNN) algorithms in decoding movment. For feature extraction were compared methods like the wavelet transform, PSD, and average band power estimates, more specifically, Wavelet Coefficient, Alpha band PSD estimates, Beta Band PSD estimates, Alpha Band Average Power and Beta Band Average Power. The results showed that the wavelet coefficients, when used individually, contributed to poor classification accuracy. When each feature vector is fed for classification, PSD had the best accuracy of all the feature vectors.

Some BCI research have found that combining several types of features leads to greater classification accuracies than using a single feature type. Jusas and Samuvel [89] focuses on the feature extraction process and proposes combining different feature extraction approaches: Band Power (BP), Time Domain Parameters (TDP), FFT and Channel Variance (CV). When two feature extraction methods are used together, the number of selected features that are redundant or irrelevant increases. As a result, while investigating approaches by combining them in pairs, a feature reduction was used. The most efficient results were obtained by combining the methods FFT and CV as feature extraction with PCA as feature reduction.

Combining numerous feature types generally increases dimensionality. The number of features is proportional to the number of parameters that the classifier must optimize. Reducing the number of features means the classifier has fewer parameters to optimize, which can enhance performance since it can usually make faster predictions and be computationally more efficient [90].

The process of selecting the most significant features to use in classification algorithms is known as feature selection. Feature selection methods are used to minimize the number of input variables by removing redundant or irrelevant features [91]. Filter, wrapper, and embedding techniques are commonly used in the machine learning literature to classify feature subset selection algorithms [92].

Filter approaches are commonly used as a step in the preprocessing process. Features are chosen based on their association with the outcome variable as measured by various statistical tests [93]. The most well-known filter methods are Pearson's Correlation, it is a metric that measures the linear dependence between two continuous variables, LDA and ANOVA (Analysis of Variance). [94].

Wrapper methods start to select a subset of features and apply them to train a model. It is determined to add or delete features from your subset based on the inferences. These methods can take a long time and are generally slow. According to the literature, Genetic Algorithm (GA) is the most used feature selection algorithm [33, 95, 96]. Yaacoub et al. [97] used a new feature selection method that uses genetic algorithms to improve left-and right-hand movement recognition. The suggested strategy minimize the number of features to as low as 0.5% (i.e., the number of discarded features reach 99.5%) while improving the classifier's accuracy, sensitivity, specificity, and precision, according to experimental data, obtaining better outcomes than simply using the classifier. Forward feature selection, backward feature elimination, and recursive feature elimination are common techniques in wrapper methods. Forward selection is an iterative method that begins with no features in the model and gradually adds them until the model's performance is unaffected by the addition of new ones. Backward elimination begins with all of the features and eliminates the least significant feature at each iteration, repeating this process until no improvement in the model is detected. Recursive feature elimination iteratively generates models, retaining the best or worst performing feature at each iteration. It builds the next model using the features that are left until all of them have been used up [94].

Embedded approaches inbuilt feature selection, which allows a classifier to create a model that performs attribute selection automatically as part of the training process (performs feature selection and

model fitting simultaneously) [98].

2.2.3 Classification

Decoding human locomotion intentions may be achieved using either regression or classification methods, however classification techniques are presently the most popular approach [54]. In a BCI system, the classification goal is to recognize a user's intentions using a feature vector that identifies the brain activity provided by the feature extraction and selection steps.

There are two types of classification algorithms: conventional Machine learning (ML) algorithms and DL algorithms [99]. Conventional ML is used in the majority of BCIs, mainly in the early decades, although DL approaches are exponentially growing. Recent studies have reported that employing DL techniques rather than ML improved model accuracy.

Both types of ML can be categorized as supervised and unsupervised. Most biomedical research employs supervised classification. Supervised learning is a type of machine learning that makes use of labeled datasets. The algorithm learns from the training dataset by making data predictions and adjusting to achieve the proper response. Unsupervised learning is a type of machine learning that analyzes and clusters unlabeled datasets, working on their own to discover the inherent structure of unlabeled data [100].

Conventional Machine Learning This is the most popular method, and several algorithms have been developed to decode human movement intentions. Linear classifiers gather discriminant classifiers that use linear decision boundaries between the feature vectors of each class. They include LDA [24, 101] and Support Vector Machine (SVM) [6, 28, 101]. Both LDA and SVM were, and still are, the most popular types of classifiers for EEG based-BCIs, particularly for online and real-time BCIs. Algorithms like Bayesian analysis, KNN and ANN are also found in the literature.

Schlögl et al. [102] evaluate and compare the performance of several classifiers of four-class motor imagery EEG data. For this purpose, they perform LDA, for single-channel analysis and LDA, KNN and SVM for multi-channel analysis. Topographic maps were created using the single-channel results, revealing the channels with the highest level of separability across classes for each subject. The results of multi-channel algorithms show that SVM is the most successful classifier, whereas KNN is the least effective.

Deep Learning Although traditional classification algorithms have proven quite efficient in evaluating large data sets and understanding the relation between variables, when highly dynamic features are identified, they generally lead to poor generalization behavior and low classification accuracy [103]. Additionally, due to a high delay time, there is a trade-off between accuracy and responsiveness [104]. When controlling real-time devices with EEG decoders, the delay time is especially important.

DL is a machine learning algorithm in which a classifier learns EEG features that relate to specific classes. There are a variety of deep learning algorithms. Convolutional Neural Network (CNN) and Recurrent

Neural Network (RNN), mainly Long short-term memory (LSTM), are the most frequently applied algorithms in movement decoding.

Dose et al. [105] developed and tested a DL approach using CNN for an EEG-MI BCI system that could be utilized to enhance current stroke rehabilitation strategies. The model reached an average cross validation accuracy of 87.98%, 76.61%, and 65.73%, respectively for the two-, three-, and four-class classification tasks. Therefore, it was concluded that deep neural networks might eventually outperform and replace existing standard algorithms if enough suitable data is available and additional advancement towards a decent network design is made.

Tortora et al. [106] developed and tested an LSTM deep neural network for dealing with time-dependent information in brain signals during locomotion. The proposed approach achieves an accuracy greater than 80% in the decoding of gait patterns (swing and stance states).

Related Work Table 4 lists the most relevant BCIs related to lower-limbs movement intention. The majority of research focused on decoding gait and standing intentions. For this purpose, Hasan et al. [6] and Hortal et al. [28] used the SVM algorithm as a classifier, achieving an accuracy greater than 70%. Choi and Kim [24] used the LDA algorithm, which proved to be more efficient than the others, with an accuracy of more than 80%. Delisle-Rodriguez et al. [101] used both LDA and SVM. Although the differences were minimal, LDA outperformed SVM. Nevertheless, SVM and other ML classifiers have limitation, such as low speed of execution [107]. In order to overcome conventional ML's limitations, Park et al. [104] propose spatio-spectral CNN with 83.4% accuracy on gait state detection using a relatively short segment of EEG data (0.2s). The accuracy of the gait/stand intention recognition, which identifies the subject's gait intention before the actual gait, was 77.3%.

A consistency of artifact removal and feature engineering approaches can also be seen in the table 4. ASR is the most widely used technique for artifact removal, whereas FFT is the most widely used method for feature engineering, particularly for feature extraction.

Table 4: Movement intention-based BCI in the literature

Research	Type of moviment	Filtering	Artifact Removal	Feature engineering	Classifier	Accuracy %
Hasan et al. [6]	gait start or stop intention	High pass FIR at 1 Hz Notch at 60 Hz	ASR ICA	DWT Hjort parameters	SVM	75.8
AH et al. [108]	Foot dorsiflexion	Band pass [0.01-50Hz]	Removal of "hat band"electrodes	FFT PSD	Linear Bayesian	85.1 to 97.6
Hortal et al. [28]	Rest and walking state	Band Pass 8th order Butterworth [5-40]Hz	Laplacian algorithm	FFT	SVM (RBF kernel)	70.5 (rest); 75.0 (walk)
Delisle-Rodriguez et al. [101]	Stand (rest) and gait planning	Band Pass [0.1-100] Hz Notch at 60 Hz	Adaptative spatial filter	FFT	LDA and LSVM	≥ 75
Choi and Kim [24]	Gait and stand transition	Band pass 3rd order IIR [3-40]Hz	ASR	CSP	LDA	82.6± 7.15
Tortora et al. [106]	Gait phases	High pass at 1Hz Low pass at 48Hz	CAR	RELICA and AMICA	LSTM	82.3±1.7
Park et al. [104]	Gait/stand intention and movement	FIR [3-40]Hz	ASR	FFT	CNN	77.3 (intention)
Bulea et al. [8]	Sitting and standing	Butterworth [0.1-4]Hz	ASR	LFDA	GMM	78.0 ± 2.6

2.3 Critical Overview

Humans' ability to walk and keep their balance is heavily influenced by gait adaptation. It is an indicator of health progression in the elderly and persons with neurological issues. As a result, assistive robotic systems should take this into account and be able to detect and adapt to variations in gait.

Because EEG signals can act as a real-time representation of the brain's motor activity during movement, EEG-based locomotion studies have a great potentiality for early prediction of future movement. However, they have also disadvantages, such as the scalp's low spatial resolution and poor SNR. Therefore, raw EEG signal is usually contaminated with many different artifacts, making the preprocessing phase essential. They can be related to the subject or be related to other external and environmental causes. To remove each sort of artifact, different approaches are employed. The use of temporal/spatial filters, artifact removal methods and feature extraction techniques improves the signal-to-noise ratio, allowing for more accurate classification. The most often discussed approaches for removing artifacts are a combination of ASR and ICA. In motion decoding, neural features such as MRCP and ERD are employed, and the most commonly used feature extraction methods are PSD and FFT. Many ML approaches have been successfully developed for the detection of movement intention using EEG. DL approaches, on the other hand, have lately proven to be more efficient, particularly for online BCIs. In all, 75% of DL research used CNN, while 36% of ML studies used a SVM to obtain competitive accuracy [103].

EEG motor-based BCI's are becoming more advanced, however, most lower-limb task research are still quite rudimentary, in the sense that they only decode relatively simple movements (i.e. walk and stand decoding), with a lot of potential for improvement. Feature extraction is the biggest challenge for decoding BCI's. It needs proper topic knowledge from researchers and can be complicated. Due to human limitations, extracted features may not be properly generalized on particular tasks.

Chapter 3

EEG based Locomotion Features

3.1 Research Plan

The main goal of this work is to develop a EEG-based computational framework that can decode a certain set of lower limb motions performed daily, such as start/stop walking, standing/walking, level-ground/stair walking, level-ground/ramp walking. The framework will be developed to perform the following consecutive stages: preprocessing or signal enhancement, feature extraction, and classification based on DL algorithms (e.g., ICA and ASR). Further, this dissertation will perform a benchmarking analysis regarding preprocessing and removal artifact algorithms, EEG features, and deep learning classifiers (e.g., CNN, LSTM, C-LSTM) to propose a reliable framework.

In this work, an open-source database was used [23] containing EEG data collected from 10 healthy participants using a 64-electrode EEG cap while walking on a circuit containing level ground, stairs, and ramps. Expected results include an accurate framework for decoding five locomotion modes (walking, stair ascent, stair descent, ramp ascent, and ramp descent) and two discrete transitions (start/stop walking, standing/walking). The framework should be robust and present a modular architecture so it can be easily integrated into different robotic platforms.

In this section are presented the EEG data processing algorithms, including filtering and locomotion-related artifacts removal techniques which were used in the final processing. It will be explored and compared the various types of filters to be utilized, as well as the frequency ranges and artifact removal techniques that are most appropriate for detecting lower limb movement. The best method to perform feature extraction and feature selection will also be analysed. For this purpose a matlab toolbox, EEGLAB, was used. Figure 8 shows the flowchart with all the steps of this process.

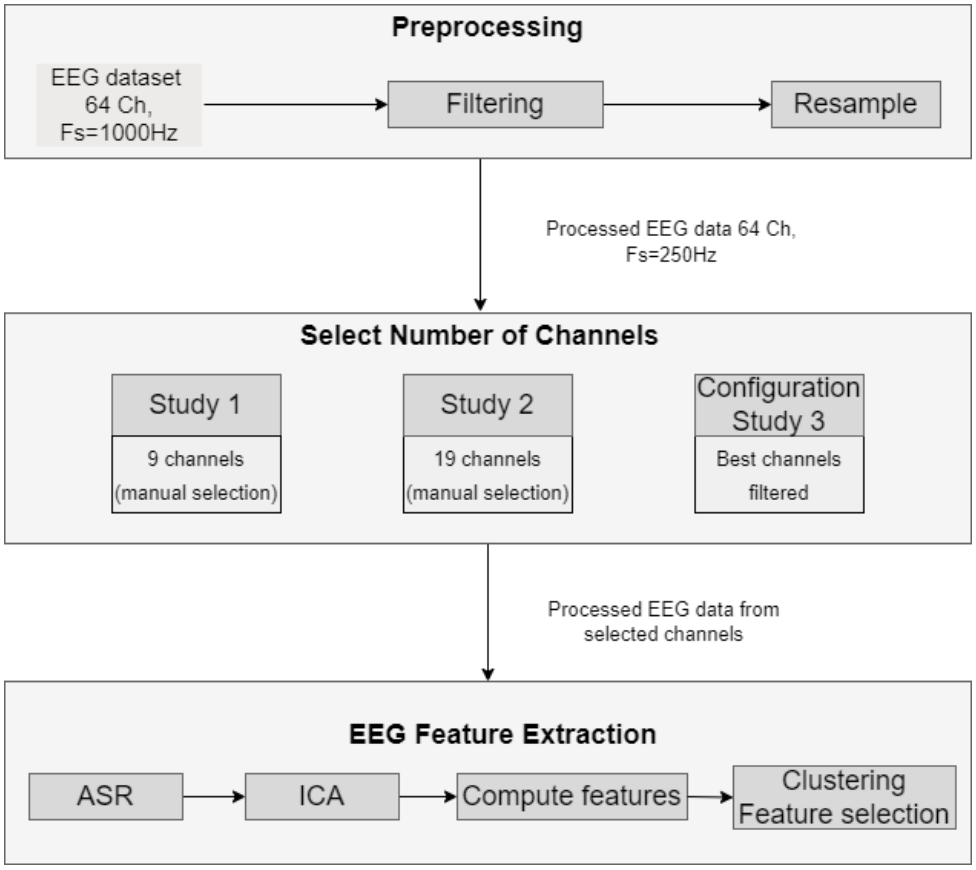

Figure 8: Compute features Flowchart

3.2 Dataset Restructuring

A 64-channel Ag/AgCl active electrode EEG setup was used to record wirelessly at 1000 Hz. Channels TP9, PO9, PO10, and TP10, associated with blinks and eye movements, were removed and excluded from the entire study.

The dataset used consists of 100 files, each one representing a trial of a given subject. Overall, 10 subjects were used, performing 10 trials each. Each trial is composed of a custom-built gait course with five stable locomotion modes: level ground walking (LW), stair descent (SD), stair ascension (SA), ramp descent (RD), and ramp ascent (RA). Figure 9 shows the gait course setup used for this data collection.

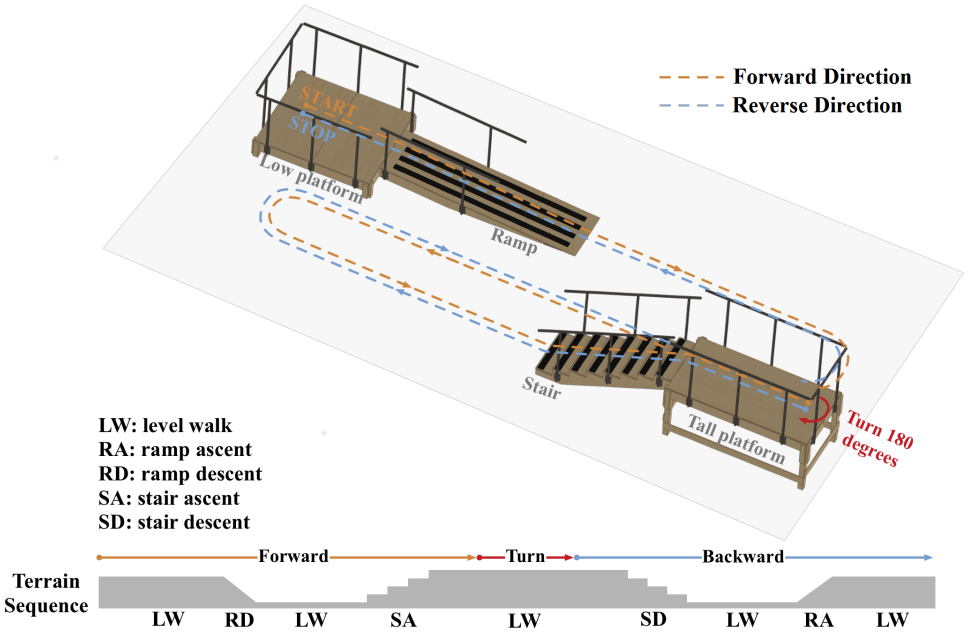

Figure 9: Gait course setup

Since this study will focus on identifying and classifying the data according to the terrain type, and in order to simplify the subsequent feature creation process, a restructuring of the datasets was initially done.

To accomplish this, each dataset was subdivided by the five types of locomotion mode, with the terrain transition parts of the signals discarded. However, as the next steps were carried out we came across some errors that came from the fact that some datasets were too small, not allowing to perform certain tasks. To deal with this problem, it was then necessary to group datasets. In this case, all trials of the same locomotion mode were grouped together for each subject. To better understand this manipulation of the dataset structure, a scheme of the entire process is shown in figure 10.

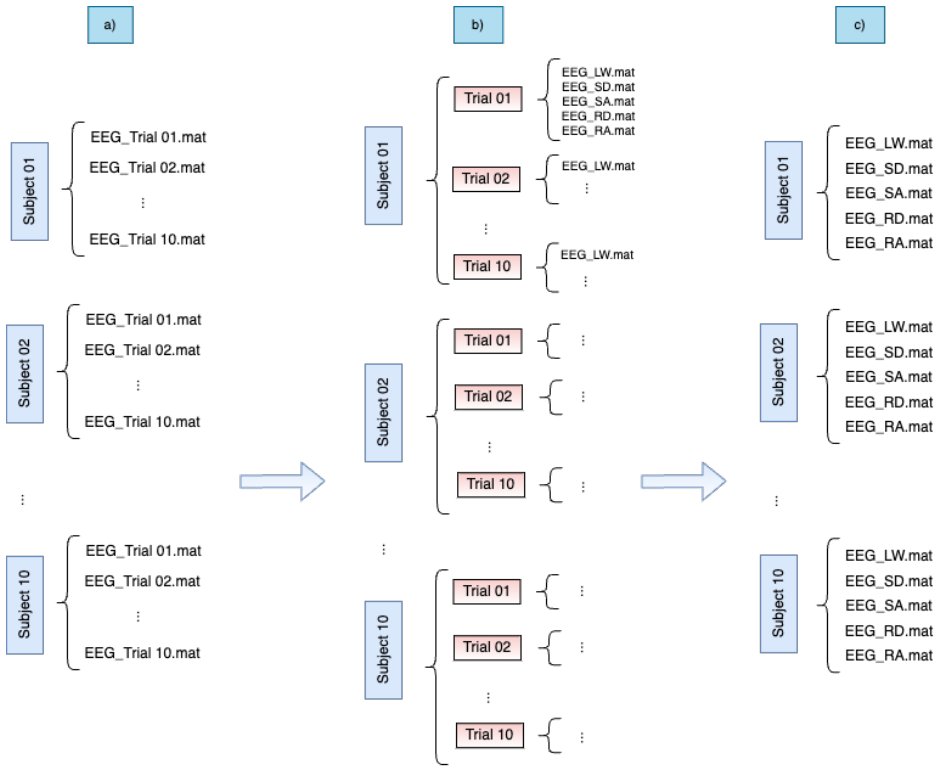

Figure 10: Flowchart

3.3 Filtering

Data should be pre-processed in terms of filtering and artifact removal before using the EEG for further analysis. Filters are needed to select the frequency band of interest as well as to remove noise that affects the quality of the signals.

Three different types of filters were studied for this purpose. In eeglab, a hamming windowed sinc 826th order FIR filter is the standard filter that is employed. As an alternative, a zero-phase 6th order digital filter is also provided (Infite Impluse Response). However, as described in section 2.2.1, the butterworth type filter (4th order) was the most widely used in the literature [8][28], so it was important that this was also included in this study. Thus, the filters to be compared are the FIR and IIR filters already provided by EEGLAB, as well as the butterworth filter.

To begin with, it was necessary to determine the frequency range that we were going to use in the study. Based on the literature study, the high cutoff value was set at 40Hz. The low cutoff value should be as close as possible to 0Hz. However it is necessary to consider the state of the data collected. Low-frequency noise can negatively affect the quality of the signal by introducing fluctuations and drift, particularly when the EEG is being used while the subjects are moving. As a result, in this context, a low cutoff frequency must be chosen while taking into account a compromise between noise reduction and the use of a low-frequency signal. Therefore, the low cut off value was tested for three frequencies, being these, 0.1, 0.5 and 1. For

this, the FFT for each type of filter was calculated using the signal from trial 1 of subject 1.

Using zero-phase digital IIR filter with a frequency cutoff range of [0.01 40] will convert all data to NaN values. Since it was difficult to evaluate and compare this filter, it was immediately excluded from the study, focusing only on the other two.

The sampling rate was reduced from 1000Hz to 250Hz in order to increase computation speed without losing any relevant information

3.4 Select Number of channels

One of the objective of the present work was to determine the influence of the number of channels and its location to the classification. For this purpose we carried tree studies selecting different channel combinations.

The process was subdivided into 3 studies, where for each of them a different set of channels was selected. The selection of channels from the first two studies is straightforward. The choice of channels is based on the literature, presented earlier in the section 2.1.2. The third study, on the other hand, involved more work, where the selection of the channels comes from the result of multiple steps in order to obtain only the highest-quality channels.

In **first study** the 9 main channels of the sensorimotor area were selected, these being: *F3, Fz, F4, C3, Cz, C4, P3, Pz, P4*, as shown by the figure 11

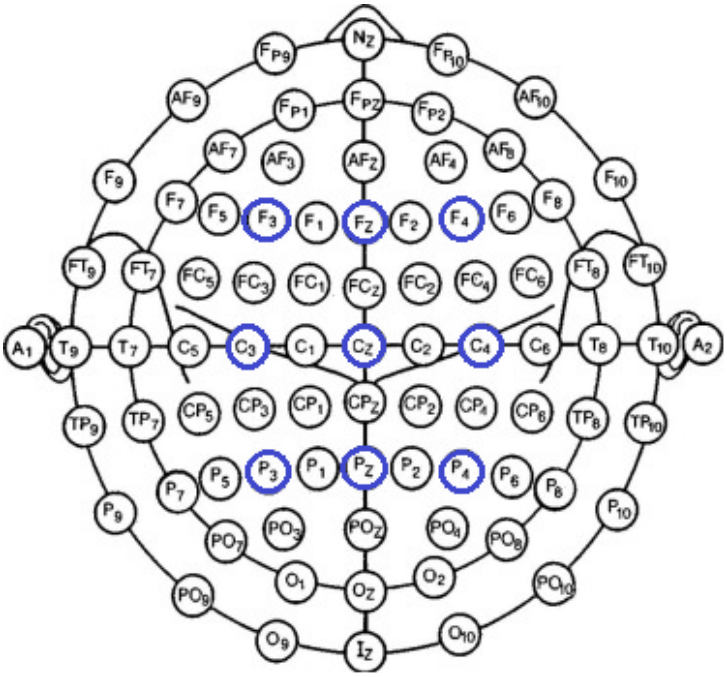

Figure 11: EEG electrodes placement- 9 channels filtered for study 1

The **second study** focuses on the same area but employs more channels. With this, we are able to understand how the quantity of channels affects the study's accuracy. Thus, the following 19 channels, shown in the figure 12, were employed for the second study: *FC3, FC1, FCz, FC2, FC4, C3, C1, Cz, C2, C4, CP3, CP1, CPz, CP2, CP4, P3, P1, Pz, P2, P4*

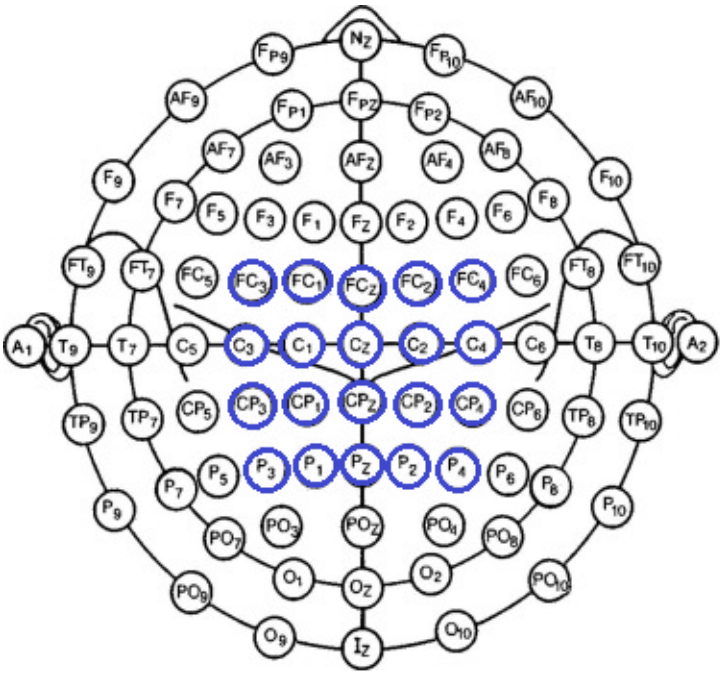

Figure 12: EEG electrodes placement- 19 channels filtered for study 2

The third study, as mentioned above, required more time and effort. The goal of study 3 is to have the greatest number of channels with high signal quality. Thus, an analysis of the signals concluded that there were many channels that were affecting the signal processing. A procedure has been created to remove channels that are considered noisy:

1. Remove noisy channels: Three methods are used to remove bad channels. Flat channels, channels with a large amount of noise, and channels which are poorly correlated with other channels were rejected. It was necessary to continue processing the data since it was not entirely reliable after this step. The component map produced by ICA was examined in order to determine whether the channels had been appropriately filtered. Figure 13 represents the result of this first step.

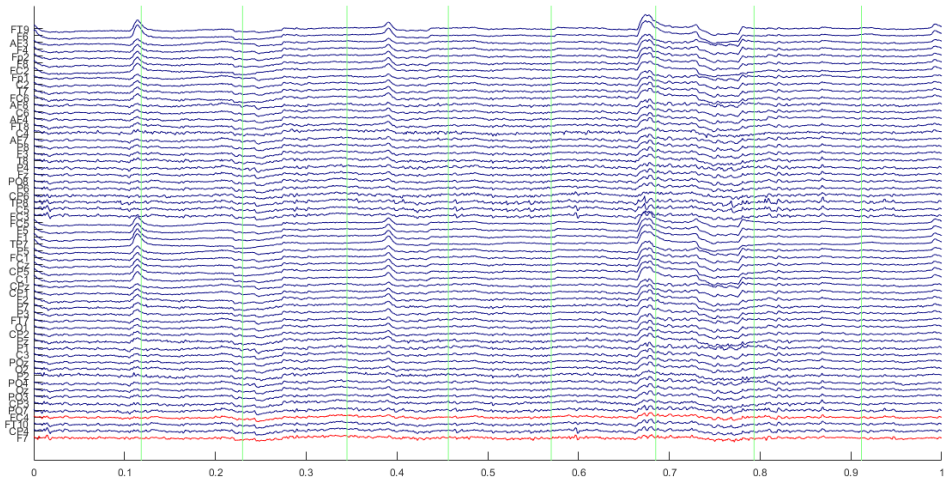

Figure 13: Scrolling data window with rejected channels highligthed

2. Artifact Subspace Reconstruction: ASR can be used to eliminate or correct inaccurate parts of data. This step is also included in the workflow for data processing that is described in section 3.5.1.

3. Remove noisy channels: Next, step 1 was performed again. This time, whereas the first step deleted 1 to 6 channels, this step removed around 20 channels. This step is also represented in figure 14.

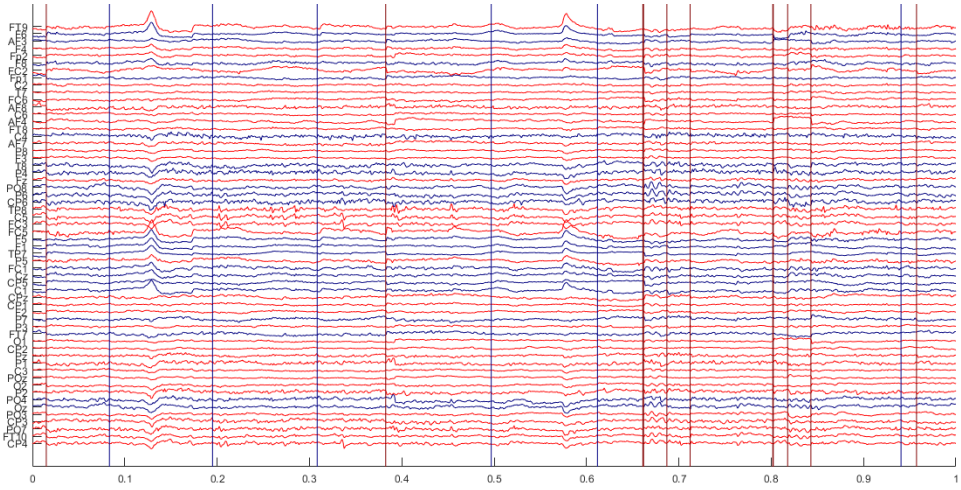

Figure 14: Scrolling data window with rejected channels highligthed by second time

It should be noted that all the processes presented above were used only to find the best channels, i.e. the data on which the study will follow did not pass through them.

3.5 Feature Extraction

3.5.1 ASR

The following method is the ASR. ASR is identical to PCA-based methods in which channel data is reconstructed from remaining components after large-variance components are removed. The main difference is that ASR uses clean data segments to calculate thresholds for rejecting components by automatically identifying and utilizing them.

ASR can be used to remove or correct bad parts of data. Removing them, which corresponds to the default parameters, is the most advisable for offline EEG processing. Overall, ASR identifies clean data (calibration data) and computes the standard deviation of the PCA-extracted components (ignoring physiological EEG alpha and theta waves by filtering them out). It discards data areas that are more than 20 times (by default) the calibration data's standard deviation. The lower this threshold, the more aggressive the rejection is. Based on the analysis of different SDC values, we came to the conclusion that the standard deviation cutoff with a value of 7 was the best choice.

Figure 15 represents the EEG signals processed by the ASR algorithm. The figure presents in highlighted red the corrupted parts of the signals that were removed.

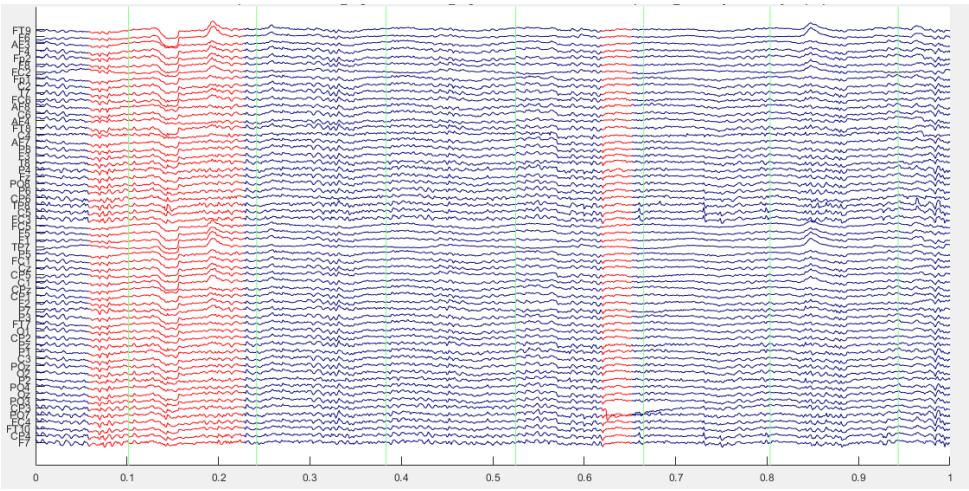

Figure 15: Data correction using the ASR algorithm

3.5.2 Extracting data Epochs

EEG epoching is a process that extracts certain time frames from the continuous EEG output. These time periods, also known as "epochs,"are typically time-locked in relation to an event.

These data epochs that are time-locked to important events must be extracted in order to analyze the event-related EEG dynamics of continuously recorded data. Therefore, this step was important so that it was possible to obtain the features related to the gait cycle.

For the implementation of this method, it is necessary to define the epochs limits and time-locking event types. The epoch limits used was the interval [0 1]s to be in line with the time of the gait cycle. Being already the default option, all the events present in the datasets were used.

Subsequently, baseline values were removed. When baseline differences between data epochs (such as those resulting from low-frequency drifts or artifacts) are present, it is beneficial to remove a mean baseline value from each epoch.

3.5.3 ICA

The ICA approach is well suited for accomplishing signal source separation when the sources are statistically independent, ie, ICA separates raw EEG data into independent sources. It is expected that the number of independent signal sources equals the number of channels.

Without eliminating the contaminated data sections, ICA can be used to remove/subtract artifacts (such as muscle, eye blinks, or eye movements) embedded in the data. Another application for ICA is identifying brain sources. Therefore, in order to remove these types of artifacts and filter the components associated with brain activity, the next step was to run the ICA algorithm, *runica*, that is the default function option. As can be seen in image 16, the 19 channels present in the signal have originated 19 distinct components that compose it.

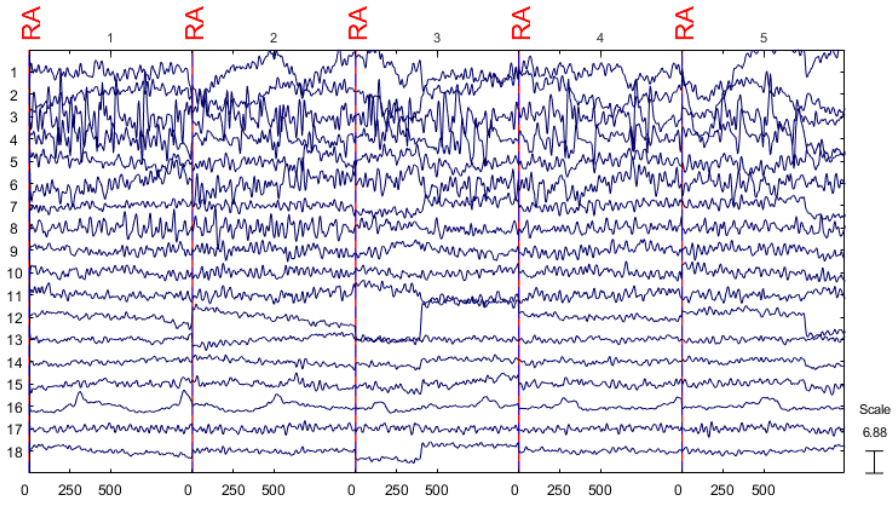

Figure 16: ICA decomposition

The most practical way to analyse the results obtained by ICA is through scalp topographies. The Scalp Topographies shows the effects that different components have on each electrode. A color scale is used to illustrate the effects of ICs, with green representing no effect and red and blue representing positive and negative contributions, respectively.

To assist in the labelling process, eeglab has a classifier, ICLabel, which classifies each of the components as being of type brain, muscle, eye, heart, line noise, channel noise and if it does not fit any of the above, it is classified as 'other'.

Figure 17 a) shows an example of a ICA components scalp map result after the data has been processed. By selecting one of them, a new figure with more details about the selected IC is displayed, as illustrated in figure 17 b). This includes graphics such as the scalp map, the component time course, the component activity power spectrum and root mean-square average projection (RMS uV).

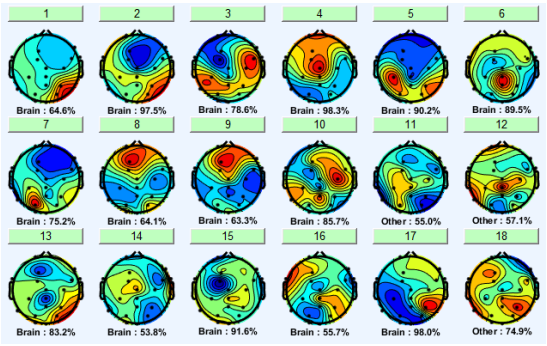

(a) Scalp map of all computed components

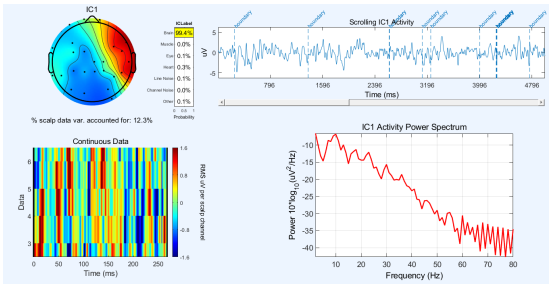

(b) Detailed window of one component

Figure 17: ICA results

Through all this data it is easy to see the pattern between the label assigned and the distribution of the data in the different plots. The primary characteristic of brain components is that the scalp topography typically appears dipolar, indicating that they have a positive potential on one side of the corresponding current dipole and a negative potential on the other. Additionally, the power spectrum narrows as frequency increases, with 10 Hz (alpha frequency) being the most prevalent.

Due to all the previous data processing steps, at this stage the artefacts detected by ICA were rare. However, it was possible to identify some in the initial steps, and the most common ones found in the datasets were muscles, heart, eyes movements and line noise. All these types of sources are represented in table 18, showing the associated sclap map and power spectrum plots.

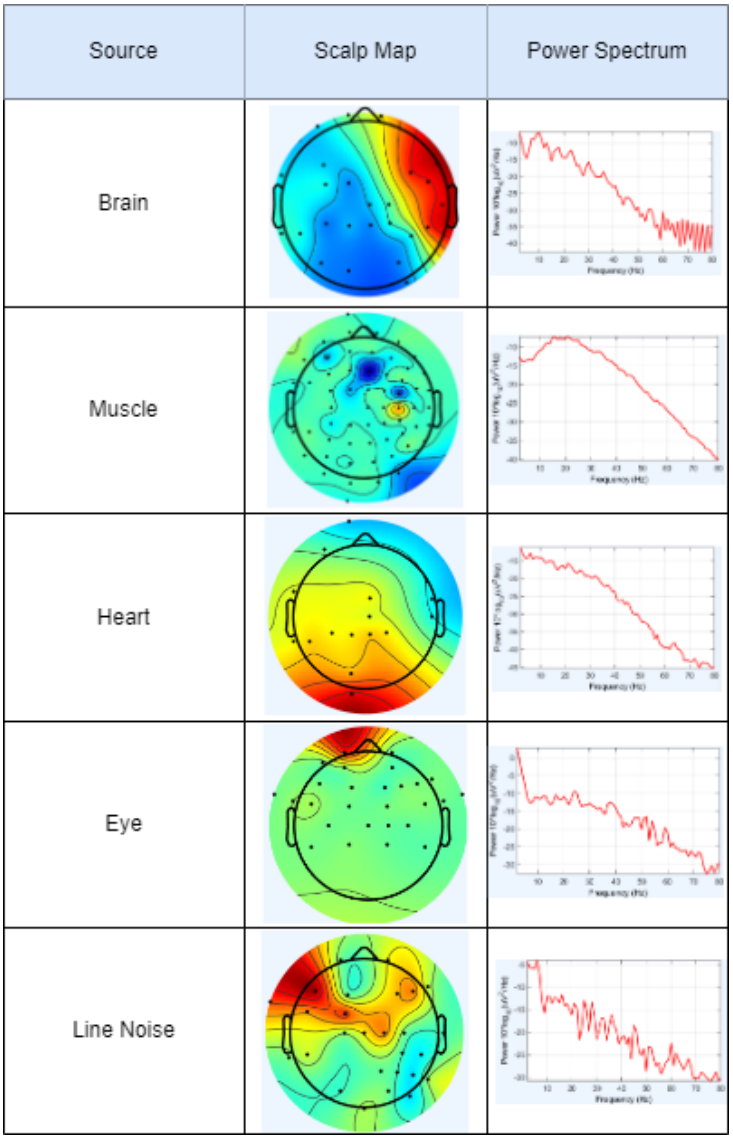

Figure 18: ICA sources

3.5.4 Compute Features

The next step is to compute component activity measures for each dataset. This required the creation of a eeglab STUDY for each of the 3 studies. A STUDY is used to manage and process data recorded from multiple subjects, sessions, and/or conditions of an experimental study. Sessions are utilized when the data is collected on different days or when a break happens that requires removing the EEG cap, which does not exist in the dataset so this field is not used. The conditions represented each file's condition, which in this case are the five types of locomotion modes. All the datasets present in the study were then loaded, specifying the information regarding each one, in this case, to which subject it belongs and the condition, in this case, gait type, it corresponds to.

After the study set up, it was first necessary to perform the process of precomputing measures.

They are required to cluster components, but they are also needed to visualize component activities. EEGLAB allows to precompute measurements such as Event Related Potentials (ERP)s, event-related potencials, Power Spectrum, spectral decomposition, Event-related Spectral Perturbation (ERSP)s, event-related spectral perturbation in the form of event-related spectral power changes and ITCs, event-related spectral perturbation in the form of event-related phase consistencies. In this step all the measures were selected.

3.6 Clustering Feature Selection

Clustering ICA components is used to interactively preprocess, cluster, and then view the dynamics of ICA signal components over one or many subjects.

In EEGLAB, the PCA clustering approach is the main method for clustering components. But first, it is important to build a preclustering matrix. The goal of this preclustering is to create a global distance matrix that specifies distances between components for use by the clustering algorithm. The condition means used to generate this overall cluster distance measure can be chosen from the previous measures. You may also enter a relative weight, which specifies the importance you want to assign to each component. In this step, all measures were used and with the same weight.

Then the clustering algorithm is applied. There are several algorithms available: kmeans, neural network, and affinity clustering. It was decided to use the default algorithm, i.e. kmeans. For its execution, it only needs to pass the number of clusters we want to create, in this case, it was 7. This choice came from the fact that this is the number of brain divisions. However, for the 9-channel study, it became more effective to decrease this value to 5, since with the initial value, the number of dipoles per cluster was very low.

The feature selection was made with an analysis of the dipoles plot of each cluster computed. A manual selection was made by choosing the cluster that held the dipoles in the target region. Then, three types of features, power spectrum, ERP and ERSP, of the chosen cluster are extracted.

3.7 Results and Discussion

In order to find the best data processing to obtain the most efficient features to be used for the classifier which differ in the number and location of the channels used.

First the filtering process will be presented, where two types of filters are compared, FIR (deafult eeglab filter) and butterworth. In addition, the low cutoff value will be compared, between the values 0.1, 0.5 and 1. The results obtained by ICA for each of the studies are analyzed below. For this, the images with the scalp maps of each component were generated. Finally, the different features produced at the end of the entire processing will be presented, including the spectrum, ERP, and ERSPs.

3.7.1 Filtering

Considering the two filter types and the different frequency cut-off ranges, through figures 19-24, it is shown the FFT plots of each combination.

Although we limited the frequencies lower and higher, the lower cut-off was the most critical for this analysis. Since all the filters proved to be efficient, the interval chosen was [0.1-40]Hz, as it is closer to 0, ensuring a better use of the signal. The filter chosen was Butterworth, with this decision being mainly supported by the literature and also because it allows its use in real time.

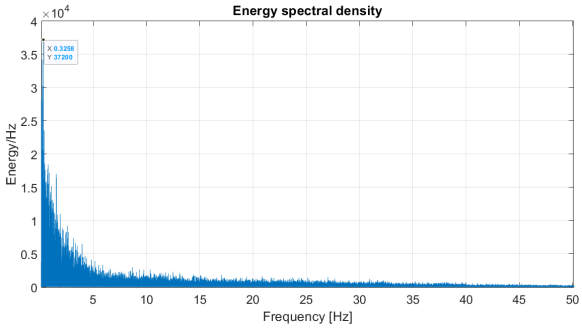

Figure 19: Butterworth [0.1-40]Hz FFT

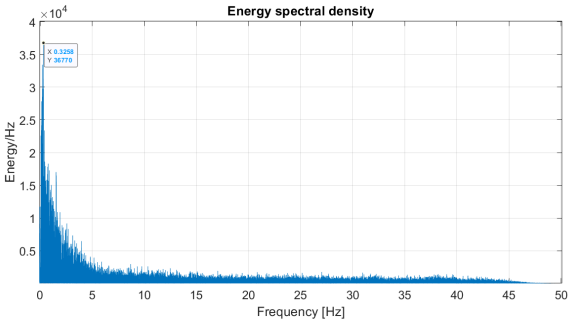

Figure 20: FIR [0.1-40]Hz FFT

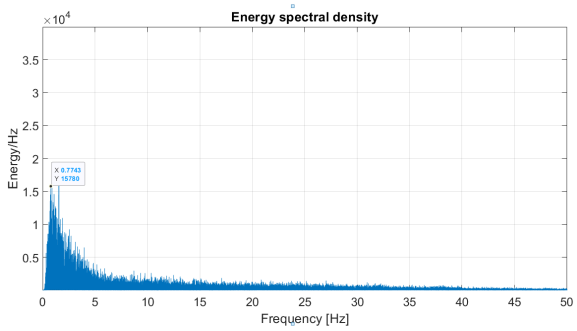

Figure 21: Butterworth [0.5-40]Hz FFT

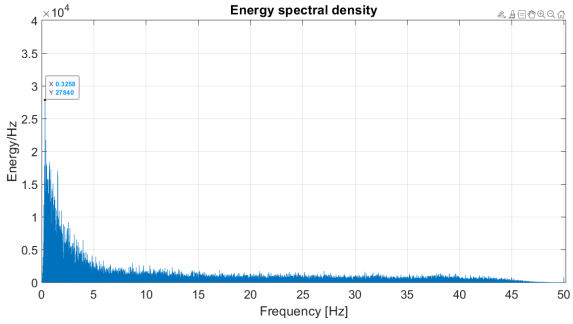

Figure 22: FIR [0.5-40]Hz FFT

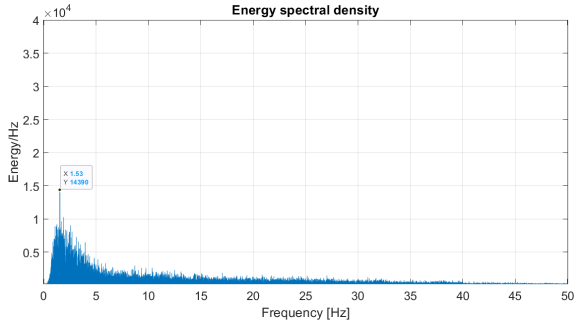

Figure 23: Butterworth [1-40]Hz FFT

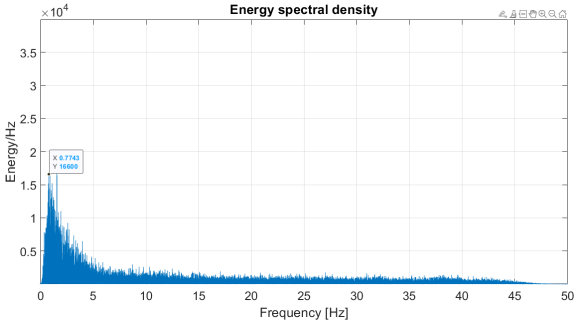

Figure 24: FIR [1-40]Hz FFT

After the filter and frequency range were selected, it was applied to the whole dataset. In the figures 25 and 26, the signal of the first three of the total of sixty channels is shown, representing, respectively, the before and after the application of the filter. It is possible to see that the data became smoother and

there was a reduction in the amplitude of oscillations.

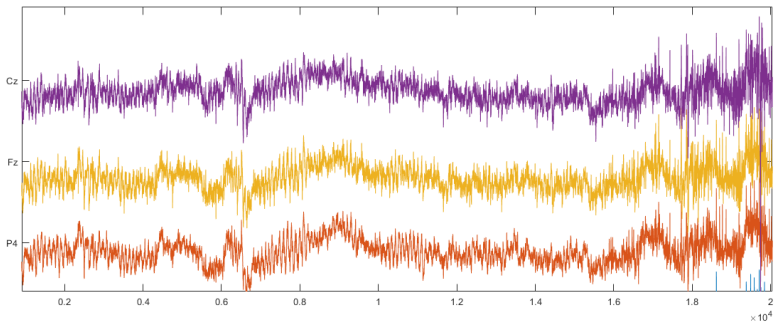

Figure 25: EEG signal before filtering

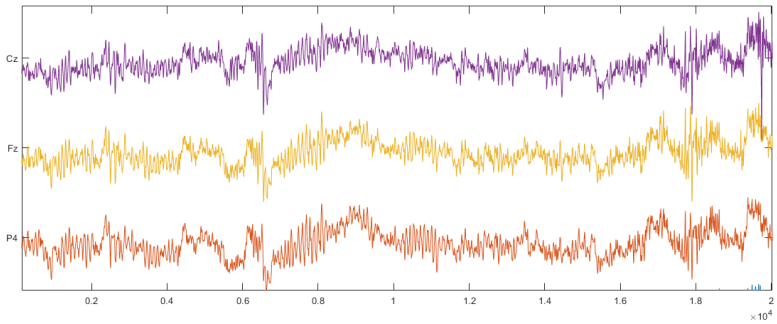

Figure 26: EEG signal after filtering

3.7.2 ICA

The ICA implementation is applied to each of the three existing studies, and is analyzed by plotting the scalp maps for each component.

There are two ways to analyze the ICA result. To determine the degree of confidence, we can first look at the percentage of each component. On the other hand, the quality of the algorithm is determined by how the components distribute their influence across the scalp. This second method of ICA evaluation involves visual inspection. Well-defined origin circles imply good processing. On the other hand, overposting and random distribution of circles suggest a worse processing.

In the first study, six components were created, of which five have been identified as brain sources. According to the estimation algorithm, processing was successful, with high brain source percentages, as can be shown in Figure 27 and Table 5.

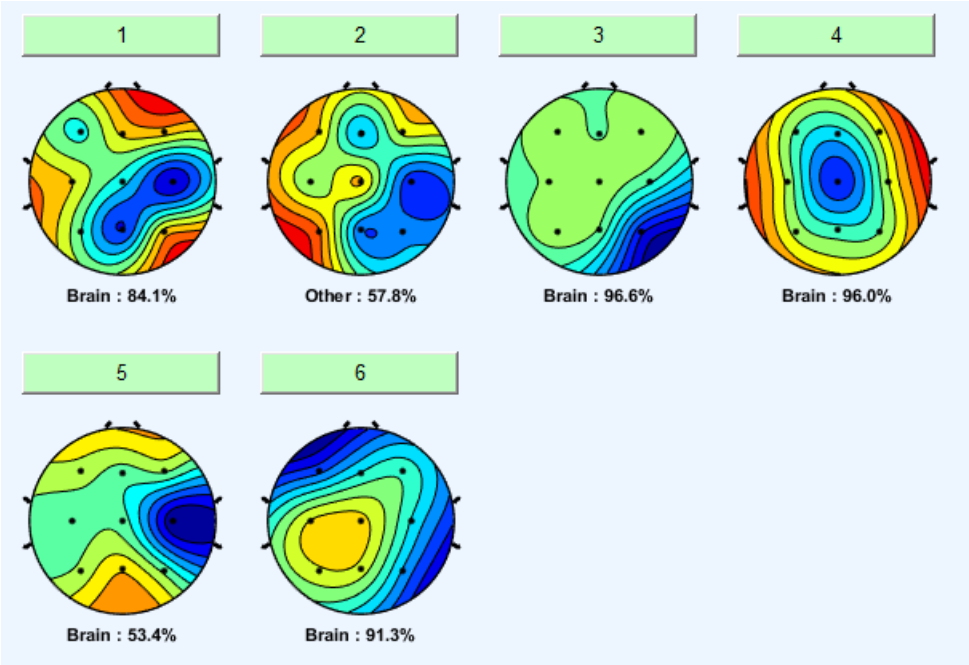

Figure 27: ICA scalp map Study 1

	Type estimation
IC1	Brain: 84.1%
IC2	Other: 57.8%
IC3	Brain: 96.6%
IC4	Brain: 96.6%
IC5	Brain: 53.4%
IC6	Brain: 91.3%

Table 5: Estimation of the type of each of the independent components for Study 1

The ICA results for Study 2 are similarly represented in Figure 28 and Table 6. In this study, 18 components were developed, with the majority of them—12—being classified as brain components.

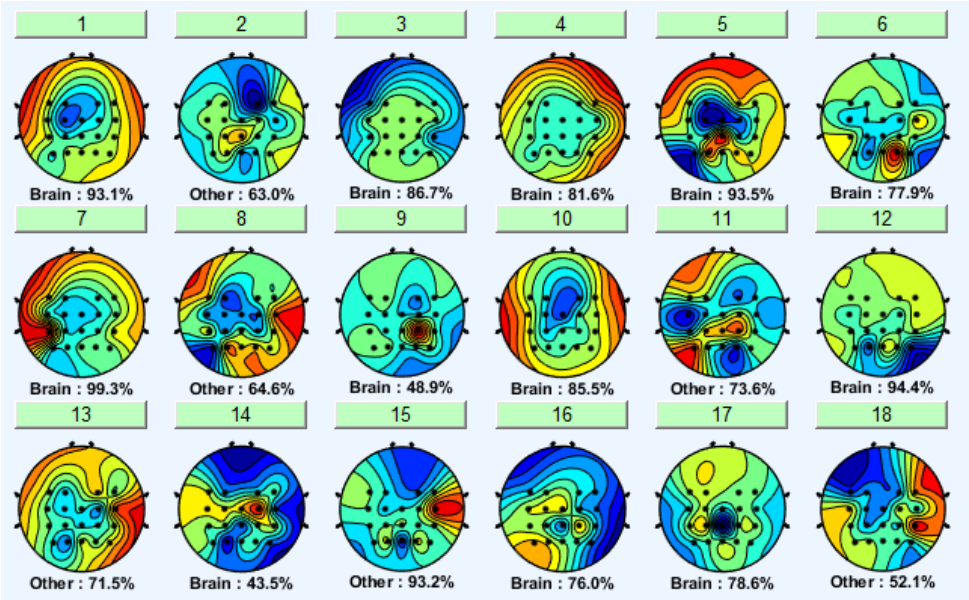

Figure 28: ICA scalp map Study 2

	Type estimation		Type estimation
IC1	Brain: 93.1%	IC10	Brain: 85.5%
IC2	Other: 63.0%	IC11	Other: 73.6%
IC3	Brain: 86.7%	IC12	Brain: 94.4%
IC4	Brain: 81.6%	IC13	Other: 71.5%
IC5	Brain: 93.5%	IC14	Brain: 43.5%
IC6	Brain: 77.9%	IC15	Other: 93.3%
IC7	Brain: 99.3%	IC16	Brain: 76.0%
IC8	Other: 64.6%	IC17	Brain: 78.6%
IC9	Brain: 48.9%	IC18	Other: 52.1%

Table 6: Estimation of the type of each of the independent components for Study 2.

The final study, study 3, revealed to have the worst results. Only 3 of the 35 created components were identified as being of the brain type. The results are displayed in figure 29 and table 7.

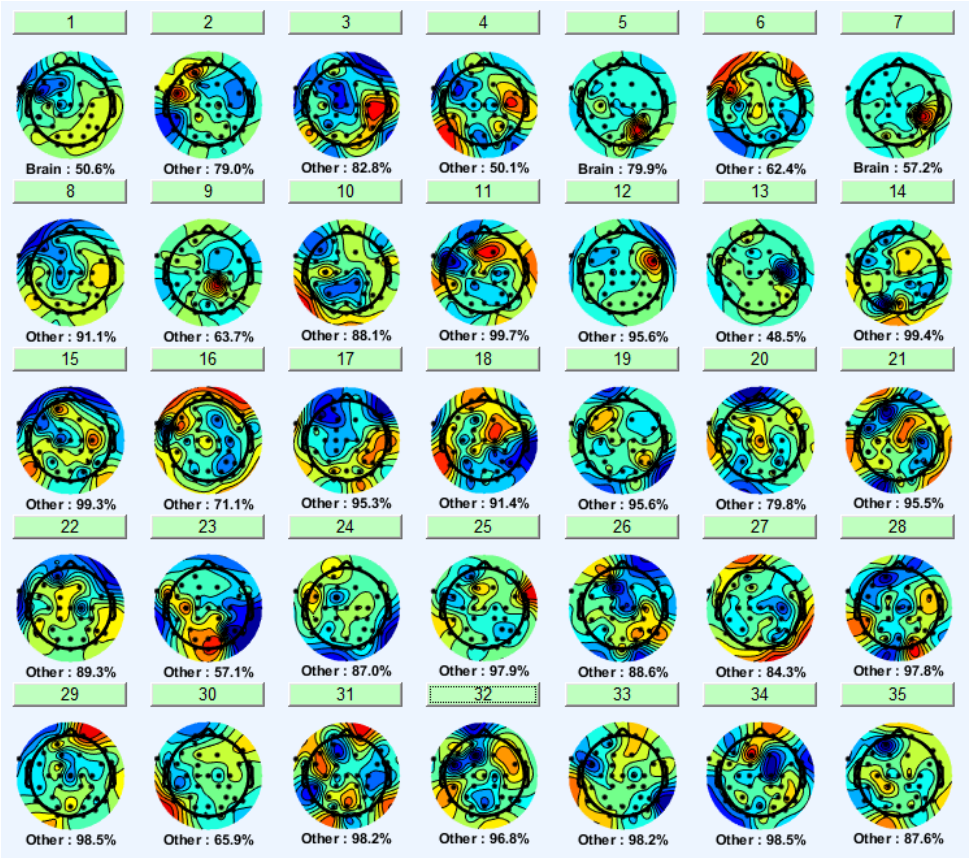

Figure 29: ICA scalp map Study 3

	Type estimation		Type estimation		Type estimation
IC1	Brain: 50%	IC13	Other: 48.5%	IC25	Other: 97.9%
IC2	Other: 79.0%	IC14	Other: 99.4%	IC26	Other: 88.6%
IC3	Other: 82.8%	IC15	Other: 99.3%	IC27	Other: 84.3%
IC4	Other: 50.1%	IC16	Other: 71.1%	IC28	Other: 97.8%
IC5	Brain:79.9%	IC17	Other: 95.3%	IC29	Other: 98.5%
IC6	Other: 62.4%	IC18	Other: 91.4%	IC30	Other: 65.9%
IC7	Brain: 57.2%	IC19	Other: 95.6%	IC31	Other: 98.2%
IC8	Other: 91.1%	IC20	Other: 79.8%	IC32	Other: 96.8%
IC9	Other: 63.7%	IC21	Other: 95.5%	IC33	Other: 98.2%
IC10	Other: 88.1%	IC22	Other: 89.3%	IC34	Other: 98.5%
IC11	Other: 99.7%	IC23	Other: 57.1%	IC35	Other: 87.6%
IC12	Other: 95.6%	IC24	Other: 87.0%		

Table 7: Estimation of the type of each of the independent components for Study 3

As we can see from the above figures, the smaller the number of channels present in the study, the

more efficient the ICA results will be. In particular, we have the last study, of the channels filtered with the eeglab methods, which did not obtain the expected results. This was due to the fact that ICA does not accept data that, for the same subject, have a number of different channels. This led to the need to implement a function that within a subject finds a number of channels that best fit a group as a whole, and the final set may not be exactly the most effective for a given subject.

3.7.3 Feature estimation

For each of the studies, the placement of the dipoles following clustering will be analyzed in this section. The cluster of interest will then be identified, and the rest of the study will be focused on that cluster. Finally, the three types of features—power spectrum, ERP, and ERSP—will be extracted for each mode of locomotion.

Using the graphs of the arrangement of dipoles after clustering, presented in figure 30, the best cluster to use in the classifier was chosen.

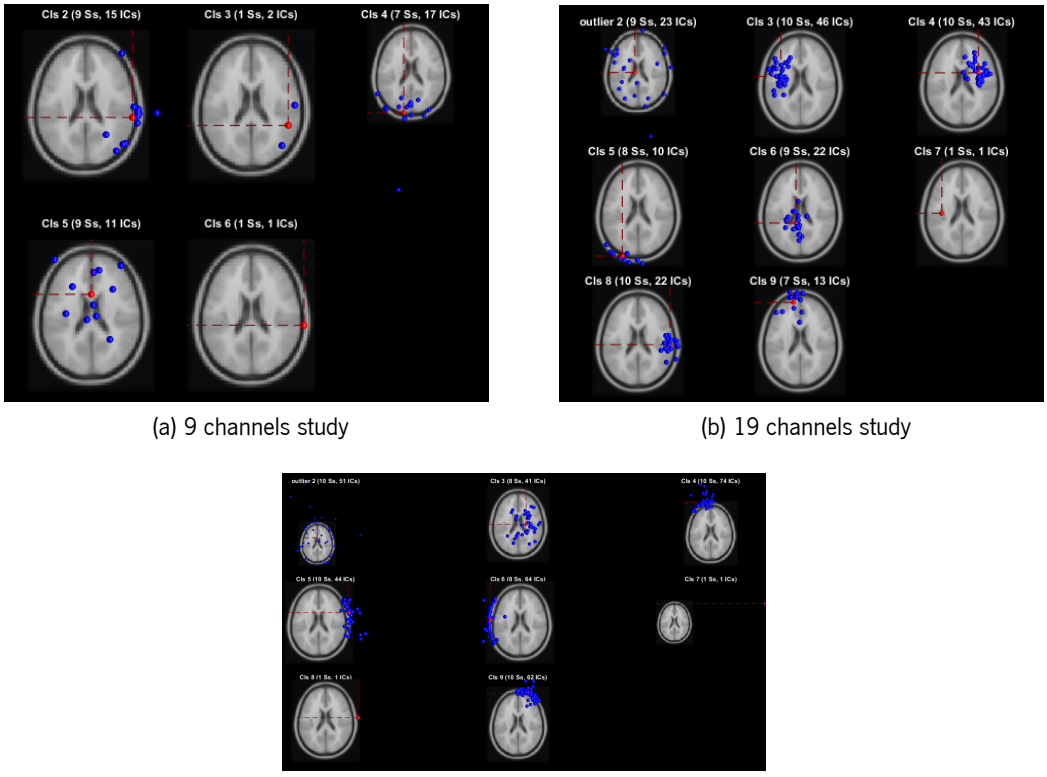

(a) 9 channels study

(b) 19 channels study

(c) Filtered channels study

Figure 30: Plot of the dipoles computed for each cluster

For the 9-channel study cluster 5 was chosen. Cluster 6 was chosen to for 19 channels study. And finally, for the last study the cluster chosen was cluster 3.

After selecting the cluster, the features to be used by the classifier were extracted. Each of these features, spectrum, ERP, and ERSP, is represented in figure 31. By analyzing each of the graphs, it can be noted that the spectrum feature is the one that changes the least according to the locomotion mode. On the other hand, in both ERP and ERSP features it is possible to identify significant differences by mode of locomotion.

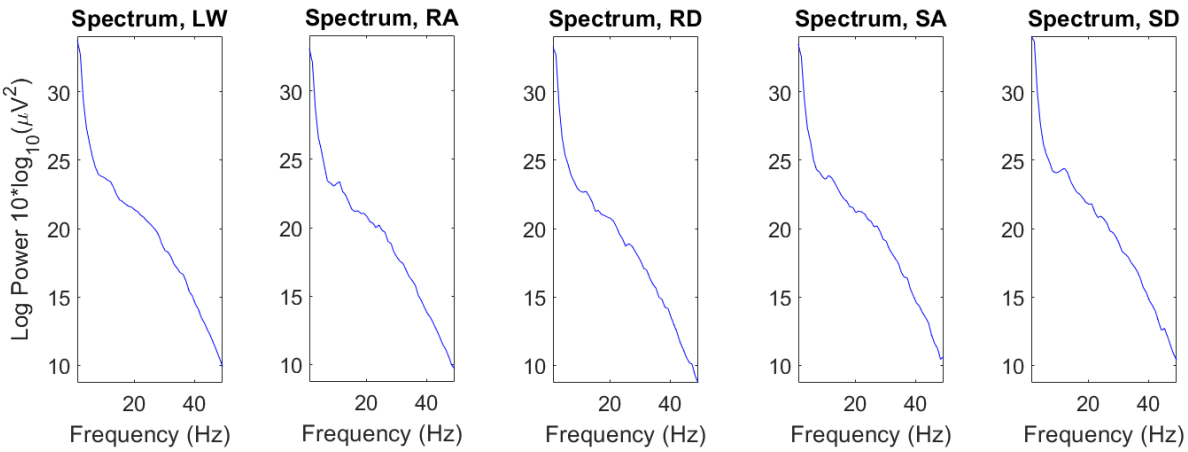

(a) Spectral plot for each locomotion mode

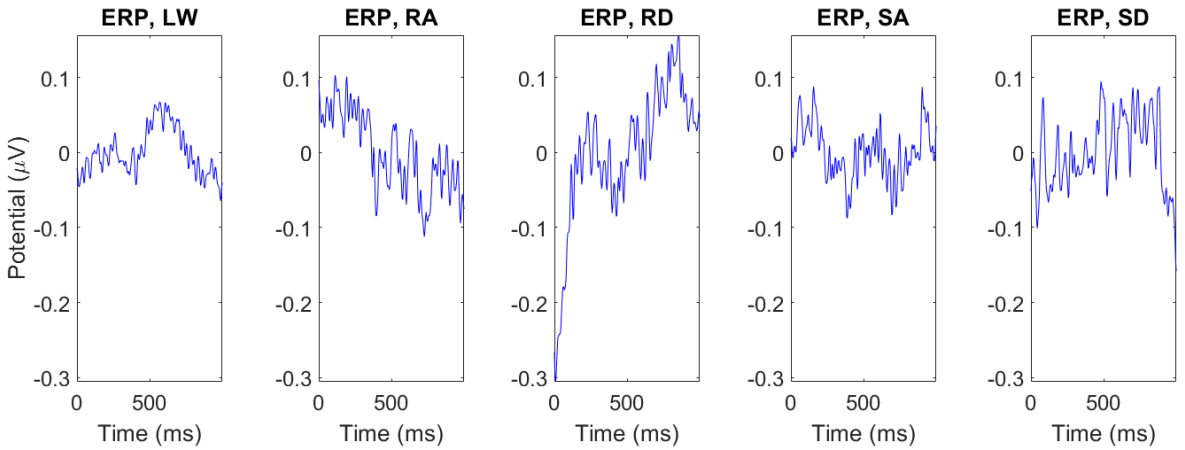

(b) ERP plot for each locomotion mode

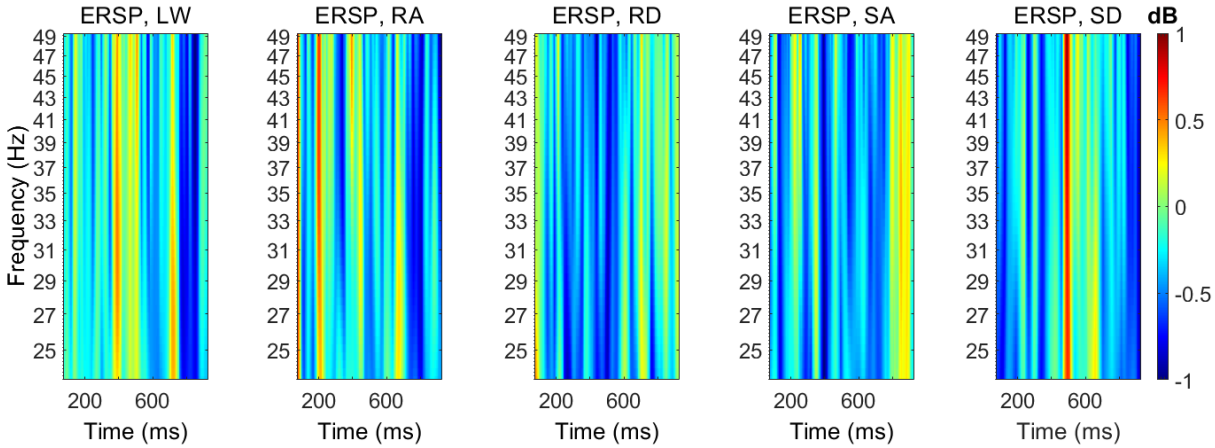

(c) ERSP plot for each locomotion mode

Figure 31: Final computed features of Study 2

Chapter 4

EEG-based locomotion mode decoding

4.1 Introduction

Finally, we have the process of classification. For this purpose, three types of deep learning classifiers were used: CNN, LSTM, and C-LSTM. This chapter will present each of the models corresponding to each classifier.

This way, for each of the studies, each classifier will use each of the 3 types of features previously obtained and then do a complete analysis to evaluate the different variants of this study, the chosen channels, the selected features, and the implemented classifier.

4.2 Data Preparation

Before proceeding to classification, it is important to adjust the data obtained to match the type and shape of the classifier's input. Although in the previous chapter the data were divided by locomotion mode, in this phase they all had to be joined in order to obtain a single dataset. It was then important to normalise the independent variables (X), using StandardScaler method. By doing this, the value distribution is resized so that the observed values' mean is 0 and their standard deviation is 1. Additionally, the function to_categorical was also applied to the vector of the target values (y), converting it into a binary class matrix. Since the LSTM input layer must be 3D, was important to reshape the independent variables (X) too.

4.3 Deep learning architectures

This section includes the description of the architecture and characteristics of the classifiers used to build the final models.

Classification models were developed in Python using the Tensorflow library. TensorFlow is a prominent open-source library for numerical computation and deep learning.

All the models were initially built by taking the basic layer structure for each of them, with the intention that they would improve over the course of evaluation. However, the standard architectures proved to be effective, so there were no relevant changes on them.

4.3.1 CNN

CNN is known for its high accuracy in image recognition and its capacity to automatically detect main features without human intervention. However, usually, required lots of training data. There are three types of layers for a CNN: convolutional layers, pooling layers, and fully connected layers.

Convolution layer is the first layer that is used to extract the various features from the input. As parameters there is filter with value 64, which represents the number of output filters in the convolution, kernel_size equal to 1, specifying the length of the 1D convolution window, and a relu activation function. To overcome the problem of overfitting in the training dataset, a dropout layer is utilized with value of 0.3. Then a max pooling is added. This layer's main goal is to reduce the convolved feature map's size in order to reduce computational costs by reducing connections between layers. After that, a flatten layer is applied. It is used as a connection between Convolution and the Dense layers, since it converts the data into a 1-dimensional array for inputting it to the next layer. Finally the network ends with two dense layers. Dense layers are the most commonly used for output layers. The number of nodes in the final layer should match the number of classes we wish to predict for, which is five in this case. In figure 32 it is possible to see the architecture of this network.

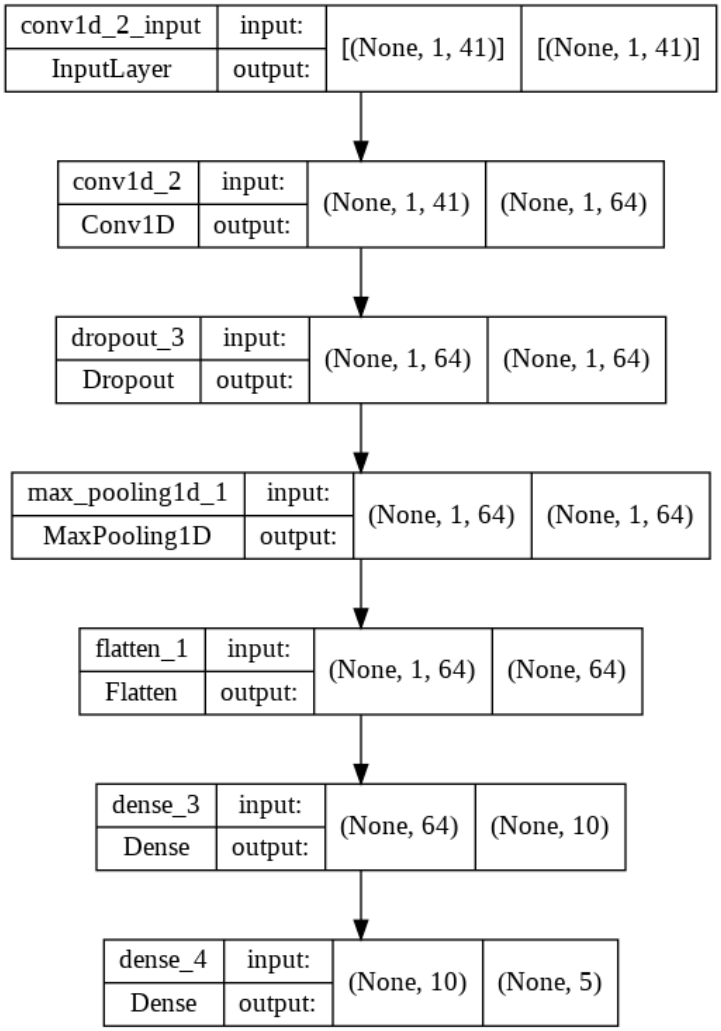

Figure 32: CNN architecture

4.3.2 LSTM

LSTM is a type of recurrent neural network (RNN) capable of handling long-term dependencies, particularly in problems involving sequence prediction. Nevertheless, LSTMs take longer to train and require more memory.

In most cases, 2 layers have proven sufficient for detecting more complex features. Although more layers may be better, they are also more difficult to train for. Since the data has already been properly processed previously, only the recommended two layers were used.

This is composed of the two lstm layers and lastly a dense layer. Between these layers, dropout layers are used to avoid overfitting problems as explained in the previous model.

Therefore, this LSTM model followed the most basic layout, as shown in figure 33

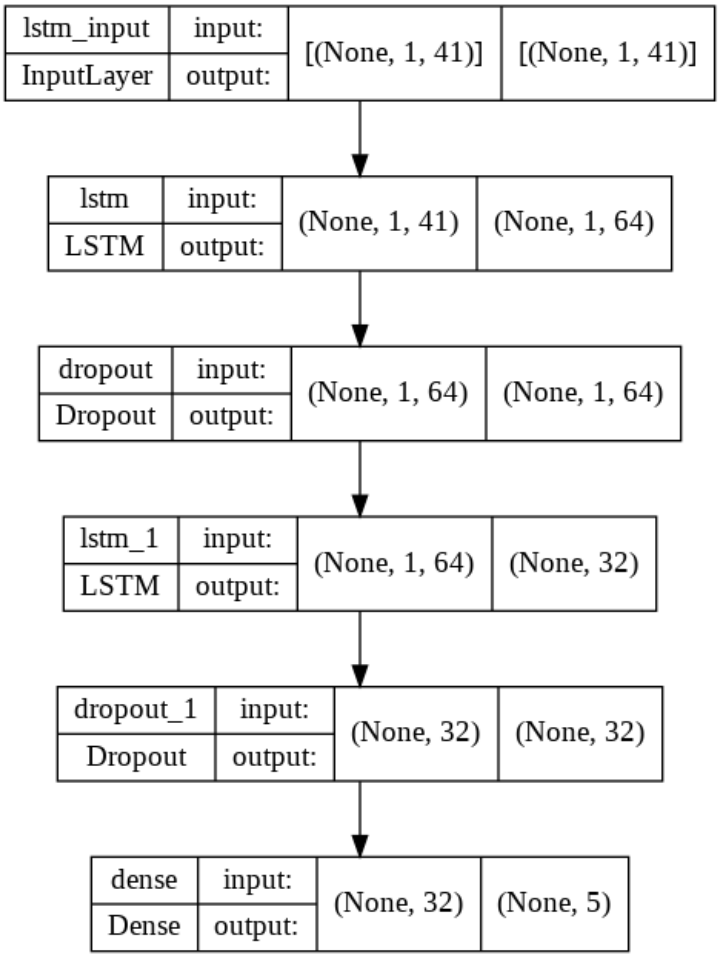

Figure 33: LSTM architecture

4.3.3 C-LSTM

In the CLSTM architecture, CNN layers are used to extract features from input data, while LSTMs are used to enable sequence prediction. This model is first composed of convolution and maxpooling layers, followed by lstm layers, and ending with a dense layer. All layers were implemented with the same parameters as the previous ones. As before, throughout the model dropout layers have been added. It is possible to see the network's structure in figure 34.

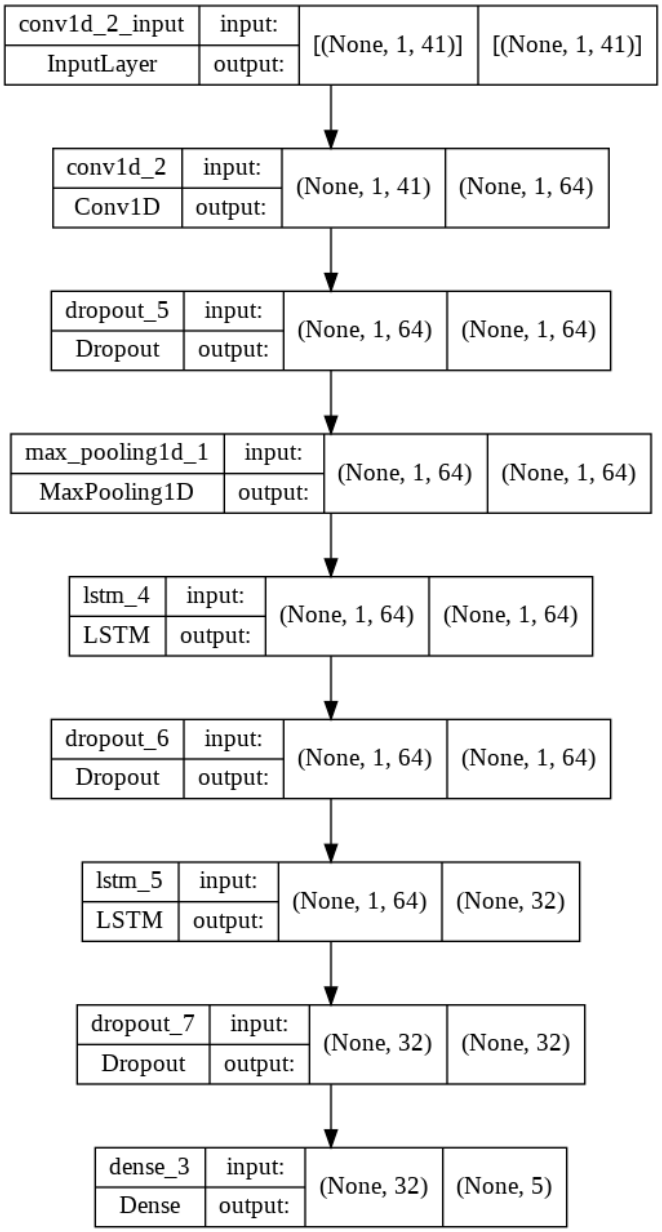

Figure 34: C-LSTM architecture

4.4 Model evaluation

Model evaluation is the practice of applying different evaluation metrics to analyze the performance of a machine learning model.

To evaluate the models, the dataset was initially splitted into train/validation dataset and test dataset. This split process was conducted with a 80:20 ratio, using 20% of the data for the test procedure which the models never use for training.

On the training data the K-fold Cross-Validation method was applied. This approach ensures that the

model's performance is independent of how we chose the train and test sets. To achieve this, the data set is split into k subgroups, and k iterations of the holdout method are performed. Given the limited input data, this is a great approach. For this particular implementation the value of k was assumed to be 10.

To evaluate the models, metrics such as accuracy, confusion matrix, Matthews Correlation Coefficient (MCC) and F1 score were used. The classification accuracy alone can be a misleading metric since it only considers correctly identified classes. Thus, when there are more than two classes or the dataset is not balanced, additional metrics such as the MCC or the F1 score should be used. The models evaluation process included the computation of all confusion matrices. Not only does it show the errors of classifier, but more crucially, it identifies the specific mistakes that are being done. Precision and recall are the are the fundamental metrics retrieve from this matrix. Precision represents the proportion of all successfully detected positive cases over all predicted positive cases, and recall is the percentage of all really positive cases that were accurately recognized as positive instances.

F1 score was the most important metric for evaluating the classification step and it is Recall and Precision's harmonic mean. Therefore, F1 score will be the metric used to present the results in the next section. However, the results corresponding to the other metrics will be presented in the appendix.

4.5 Results/Discussion

This section will first present the results corresponding to training the three different models, CNN, LSTM and C-LSTM, with each of the extracted features, power spectrum, ERP and ERSP. Afterwards, the test results for the solutions that proved to be most effective will be presented.

From figure 35, it is possible to verify that for the first study, corresponding to the study with 9 channels, the ERP and ERSP features obtained the best results. The average F1 scores per feature are 59.67%, 92.62%, and 93.01% for power spectrum, ERP, and ERSP, respectively. Thus, there is a 55.22% variance between ERP and power spectrum features, and 0.41% between ERSP and ERP features.

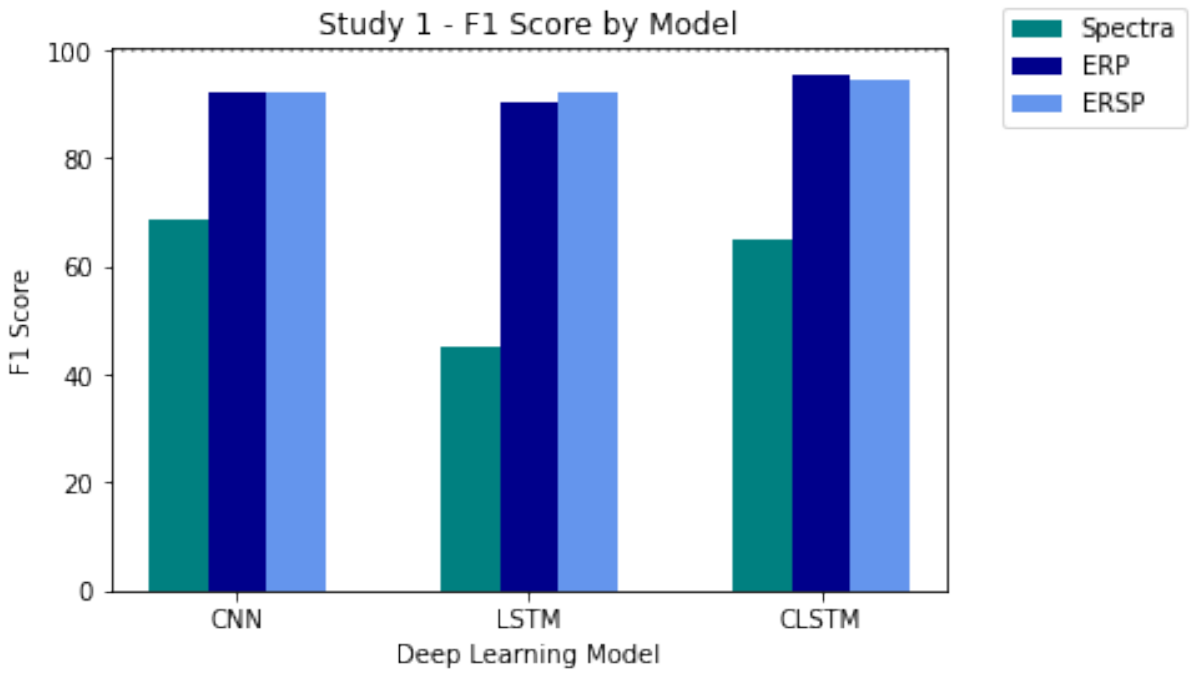

Figure 35: Study 1 F1 Score by DL model

In the second study, using 19 channels, the feature that stood out was ERP, as shown in figure 36. Compared to the first study, this feature obtained higher performance. In this study, the feature spectra achieved better results too, approaching the results obtained with the ERSPs. In this case, the average F1 scores for the features power spectrum, ERP, and ERSP are 74.26%, 98.15%, and 79.99%, where the variance between ERP and Spectra features is 32.17% and between ERSP and ERP features is 22.70%.

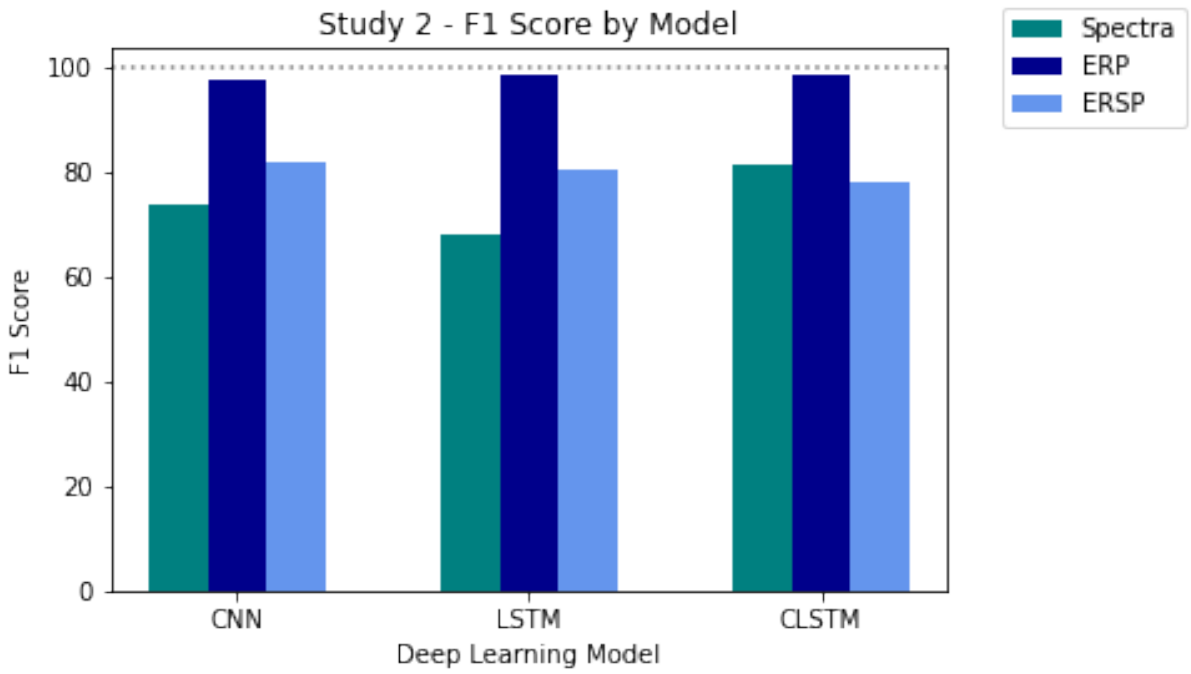

Figure 36: Study 2 F1 Score by DL model

In the last study, shown in figure 37, where the best channels were filtered according to the methods implemented with eeglab, it was where the sepctra and ERP features performed best. The average scores for the Spectra, ERP and ERSP features are 93.70, 99.83, and 74.75 respectively. So between Spectra and ERP features there is a variance of 6.54% and 33.55% between ERP and ERSP.

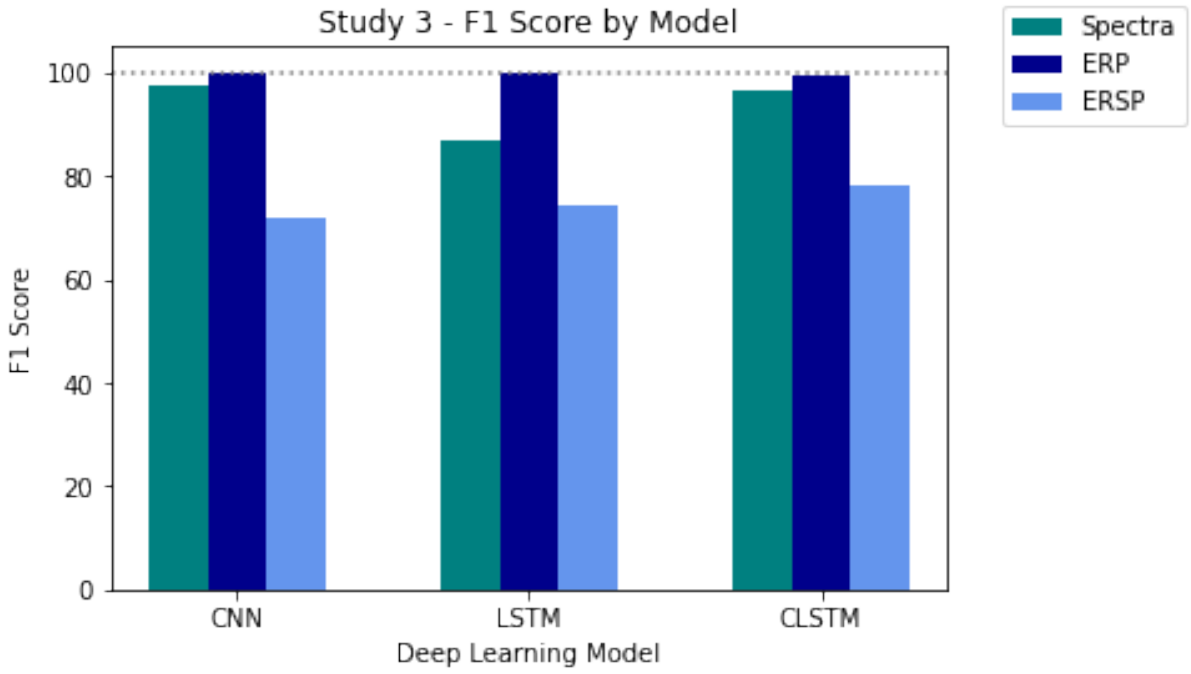

Figure 37: Study 3 F1 Score by DL model

According to the results, it can be seen that, for all the studies, the ERP feature is the most stable and with the best results, since it is connected to the potentials generated automatically in the brains of the subjects during the execution of the different modes of locomotion. In general, the results remained consistent across the three different models for the same feature, leading to the conclusion that the features had more relevance in the results than the classifier itself.

Therefore, the follow-up analysis of the classification process focused only on the ERP features. To do this, for each study a validation was performed with the test data. Table 8 presents the F1 score metric values.

	Study 1	Study 2	Study 3
CNN	86.02%	89.37%	95.99%
LSTM	85.33%	96.80%	95.56%
C-LSTM	89.55%	98.40%	99.59%

Table 8: F1 score test for each model and study

According to these outcomes, no model stands out from the others, as was already expected based on the previous results. In general, all of them obtained successful results. However, despite the small amount of variation, the study 1 obtained the lowest results, while the study 3 achieved the highest values. Again, although it is a very small difference, the classifier implemented with C-LSTM was the one that obtained the greatest scores in all three studies.

This study was not conducted considering the leave-one-subject-out cross validation method. Further experimental testing is needed to assess whether the models are robust to be used by different subjects without needing to be retrained with subject's own data.

Chapter 5

Conclusions

5.1 Concluding remarks

The work carried out in this dissertation addresses the development and validation of a DL framework based on EEG signals to decode a set of locomotion modes performed daily, namely: level-ground walking, ascending/descending stairs and ramps.

The work proposed in this dissertation was driven from challenges in literature related to the existing BCI studies for decoding motor activities. Recent literature studies suggested that the best approach to remove artefact is a combination of the ASR and ICA algorithms. On the other hand, DL approaches are achieving higher classification performance when compared to traditional machine learning approaches.

For this dissertation, an open-source database was used, containing EEG data collected from 10 healthy participants using a 64-electrode EEG cap while walking on a circuit containing level ground, stairs, and ramps. The dataset was processed considering the methods included in the developed framework, namely: (i) Filtering, (ii) ASR, (iii) ICA, (iv) Feature Estimation. Three different types of features (Power Spectrum, ERP, and ERSP) were retrieved from this process considering a noise and artifact – free dataset.

The locomotion mode decoding process in this dissertation was achieved considering three different classifiers namely: (i) CNN, (ii) LSTM, (iii) C-LSTM. The models were built and tested with the created feature set and the cross-validation results stood above 85% for all studies across all three classifiers. Furthermore, the ERP feature revealed to be the most stable across studies, and the study with higher accuracy as the study 3 with the most reliable channel selection. On the other hand, across classifiers, all three provided high performance, demonstrating reduced differences between them.

5.2 Answer to Research Questions

The work herein presented enables to answer the RQs outlined in Chapter 1.

- RQ1: Which are the best removal artifacts algorithms to yield useful EEG data from human locomotion?

  In view of what has been implemented, it is important to start by filtering the data at the frequency level and this is a very important step used by most research. Next are the ASR and ICA algorithms that identify and remove artifacts in order to filter the desired data, i.e. brain source.

- RQ2: What is the number of channels that yields the highest decoding performance? Unlike what the results of the ICA implementation suggested, the study that was shown to have better results was study 3, that is, the study where the channels were selected/filtered using data cleaning and artifact removal methods. This was the study that used the most channels. In opposition, study 1, which had only 9 channels, was the study that obtained the lowest results. Thus, taking into account the study done in this dissertation, the best range for the number of channels is between 20 and 30.

- RQ3: What is the EEG feature in the frequency domain that best represents locomotion modes? The feature that stood out as being the most effective evaluated in the classification process was ERPs. Mostly because they are related to the potentials that are automatically generated in the subjects' brains while they are performing the different types of locomotion.

- RQ4: What is the DL classifier to best decode locomotion modes from EEG data? In general, all of classifiers had excellent results. And even if by a small difference, the classifier that performed best was the C-LSTM.

5.3 Future work

Future work will be focused on the issue of the development of customized models for each subject. In this dissertation, a preliminary study was conducted to evaluate the models' capacity to classify data from subjects not previously seen in training (leave-one-subject-out cross validation). The results of this research revealed difficulties in applying the models to new subjects; hence, this issue will be researched in upcoming work. In the future, the developed models will be put to the test in real time using EEG data from a 16-channel headset (Nautilus PRO g.tec).

Bibliography

[1] M. Shah, C. Peterson, E. Yilmaz, D. R. Halalmeh, and M. Moisi. "Current advancements in the management of spinal cord injury: A comprehensive review of literature." In: *Surgical Neurology International* 11 (2020), p. 2. doi: 10.25259/sni_568_2019.

[2] C. Marquez-Chin, I. Bolivar-Tellería, and M. R. Popovic. "Brain–computer interfaces for neurorehabilitation: enhancing functional electrical stimulation." In: *Smart Wheelchairs and Brain-Computer Interfaces* (2018), pp. 425–451. doi: 10.1016/b978-0-12-812892-3.00018-2.

[3] L. van Dokkum, T. Ward, and I. Laffont. "Brain computer interfaces for neurorehabilitation – its current status as a rehabilitation strategy post-stroke." In: *Annals of Physical and Rehabilitation Medicine* 58.1 (2015). Brain Computer Interfaces (BCIs) / Coordinated by Jacques Luauté and Isabelle Laffont, pp. 3–8. issn: 1877-0657. doi: https://doi.org/10.1016/j.rehab.2014.09.016. url: https://www.sciencedirect.com/science/article/pii/S1877065714018338.

[4] M. Tariq, P. M. Trivailo, and M. Simic. "EEG-Based BCI Control Schemes for Lower-Limb Assistive-Robots." In: *Frontiers in Human Neuroscience* 12 (2018). doi: 10.3389/fnhum.2018.00312.

[5] A. H. Do, P. T. Wang, C. E. King, S. N. Chun, and Z. Nenadic. "Brain-computer interface controlled robotic gait orthosis." In: *Journal of NeuroEngineering and Rehabilitation* 10 (1 Dec. 2013), pp. 1–9. issn: 17430003. doi: 10.1186/1743-0003-10-111/FIGURES/5. url: https://jneuroengrehab.biomedcentral.com/articles/10.1186/1743-0003-10-111.

[6] S. M. S. Hasan, M. R. Siddiquee, R. Atri, R. Ramon, J. S. Marquez, and O. Bai. "Prediction of gait intention from pre-movement EEG signals: a feasibility study." In: *Journal of NeuroEngineering and Rehabilitation* 17.1 (2020). doi: 10.1186/s12984-020-00675-5.

[7] D. Liu, W. Chen, R. Chavarriaga, Z. Pei, and J. del R. Millán. "Decoding of Self-paced Lower-Limb Movement Intention: A Case Study on the Influence Factors." In: *Frontiers in Human Neuroscience* 11 (Nov. 2017), p. 560. issn: 16625161. doi: 10.3389/FNHUM.2017.00560. url: /pmc/articles/PMC5703734//pmc/articles/PMC5703734/?report=abstracthttps://www.ncbi.nlm.nih.gov/pmc/articles/PMC5703734/.

[8] T. C. Bulea, S. Prasad, A. Kilicarslan, and J. L. Contreras-Vidal. "Sitting and standing intention can be decoded from scalp EEG recorded prior to movement execution." In: ().

[9] M. Rashid, N. Sulaiman, A. P. P. A. Majeed, R. M. Musa, A. F. Ahmad, B. S. Bari, and S. Khatun. "Current Status, Challenges, and Possible Solutions of EEG-Based Brain-Computer Interface: A Comprehensive Review." In: *Frontiers in Neurorobotics* 14 (June 2020), p. 25. issn: 16625218. doi: 10.3389/FNBOT.2020.00025. url: /pmc/articles/PMC7283463//pmc/articles/PMC7283463/?report=abstracthttps://www.ncbi.nlm.nih.gov/pmc/articles/PMC7283463/.

[10] J. J. Shih, D. J. Krusienski, and J. R. Wolpaw. *Brain-computer interfaces in medicine*. Mar. 2012. url: https://www.ncbi.nlm.nih.gov/pmc/articles/PMC3497935/.

[11] M. S. GE; *A general framework for brain-computer interface design*. url: https://pubmed.ncbi.nlm.nih.gov/12797728/.

[12] W. J. N. D. G. TM; *Brain-computer interfaces for communication and control*. url: https://pubmed.ncbi.nlm.nih.gov/12048038/.

[13] S. Aggarwal and N. Chugh. *Signal processing techniques for motor imagery brain computer interface: A review*. Aug. 2019. url: https://www.sciencedirect.com/science/article/pii/S2590005619300037.

[14] S. Saad, D.-H. Kareem, and M. Jasim. "A Systematic Review of Brain-Computer Interface Based EEG." In: *Iraqi Journal for Electrical And Electronic Engineering* 16 (Nov. 2020). doi: 10.37917/ijeee.16.2.9.

[15] A. Subasi. *Practical Guide for Biomedical Signals Analysis Using Machine Learning Techniques*. Ed. by A. Press. Elsevier, 2019. doi: 10.1016/C2018-0-02414-7.

[16] B. A. M. R. GE; *A survey of signal processing algorithms in brain-computer interfaces based on electrical brain signals*. url: https://pubmed.ncbi.nlm.nih.gov/17409474/.

[17] M. B. Khalid, N. I. Rao, I. Rizwan-i Haque, S. Munir, and F. Tahir. *Towards a Brain Computer Interface using wavelet transform with averaged and time segmented adapted wavelets: Semantic Scholar*. Jan. 1970. url: https://www.semanticscholar.org/paper/Towards-a-Brain-Computer-Interface-using-wavelet-Khalid-Rao/3f736e0d8685fecb5e05153bc05bfe10eb80dd4b.

[18] *EEG vs. MRI vs. fMRI - What are the Differences?* Feb. 2021. url: https://imotions.com/blog/eeg-vs-mri-vs-fmri-differences/.

[19] D. P. Subha, P. K. Joseph, R. A. U, and C. M. Lim. "EEG signal analysis: a survey." In: *Journal of medical systems* 34 (2 2010), pp. 195–212. issn: 01485598. doi: 10.1007/S10916-008-9231-Z.

[20] M. Soufineyestani, D. Dowling, and A. Khan. "Electroencephalography (EEG) Technology Applications and Available Devices." In: *Applied Sciences* 10.21 (2020). issn: 2076-3417. doi: 10.3390/app10217453. url: https://www.mdpi.com/2076-3417/10/21/7453.

[21] A. Delval, M. Bayot, L. Defebvre, and K. Dujardin. "Cortical Oscillations during Gait: Wouldn't Walking Be So Automatic?" In: *Brain Sciences* 10.2 (2020). issn: 2076-3425. doi: 10.3390/brainsci10020090. url: https://www.mdpi.com/2076-3425/10/2/90.

[22] SleePare. *EEG for Sleep Disorders: SleePare*. url: https://www.sleepare.com/blogs/electroencephalography-eeg-sleep-disorders-diagnosis/.

[23] J. A. Brantley, T. P. Luu, S. Nakagome, F. Zhu, and J. L. Contreras-Vidal. "Full body mobile brain-body imaging data during unconstrained locomotion on stairs, ramps, and level ground." In: *Scientific Data* 5.1 (2018). doi: 10.1038/sdata.2018.133.

[24] J. Choi and H. Kim. "Real-time Decoding of EEG Gait Intention for Controlling a Lower-limb Exoskeleton System." In: *2019 7th International Winter Conference on Brain-Computer Interface (BCI)*. 2019, pp. 1–3. doi: 10.1109/IWW-BCI.2019.8737311.

[25] P. Wei and J. Zhang. "Different sEMG and EEG Features Analysis for Gait phase Recognition." In: Oct. 2020.

[26] Y. Zhang, S. Prasad, A. Kilicarslan, and J. L. Contreras-Vidal. "Multiple Kernel Based Region Importance Learning for Neural Classification of Gait States from EEG Signals." In: *Frontiers in Neuroscience* 11 (2017), p. 170. issn: 1662-453X. doi: 10.3389/fnins.2017.00170. url: https://www.frontiersin.org/article/10.3389/fnins.2017.00170.

[27] M. Elvira, E. Iáñez, V. Quiles, M. García, and J. Azorin. "Pseudo-Online BMI Based on EEG to Detect the Appearance of Sudden Obstacles during Walking." In: *Sensors* 19 (Dec. 2019), p. 5444. doi: 10.3390/s19245444.

[28] E. Hortal, A. Úbeda, E. Iáñez, E. Fernández, and J. M. Azorín. "Using EEG Signals to Detect the Intention of Walking Initiation and Stop." In: *Artificial Computation in Biology and Medicine*. Ed. by J. M. Ferrández Vicente, J. R. Álvarez-Sánchez, F. de la Paz López, F. J. Toledo-Moreo, and H. Adeli. Cham: Springer International Publishing, 2015, pp. 278–287. isbn: 978-3-319-18914-7.

[29] S. Park, H.-S. Cha, J. Kwon, H. Kim, and C.-H. Im. "Development of an Online Home Appliance Control System Using Augmented Reality and an SSVEP-Based Brain-Computer Interface." In: *2020 8th International Winter Conference on Brain-Computer Interface (BCI)*. 2020, pp. 1–2. doi: 10.1109/BCI48061.2020.9061633.

[30] B. Farnsworth. "Top 14 EEG Hardware Companies [Ranked]." In: (Apr. 2017). url: https://imotions.com/blog/top-14-eeg-hardware-companies-ranked/.

[31] N. Yahya, H. Musa, Z. Y. Ong, and I. Elamvazuthi. "Classification of Motor Functions from Electroencephalogram (EEG) Signals Based on an Integrated Method Comprised of Common Spatial Pattern and Wavelet Transform Framework." In: *Sensors (Basel, Switzerland)* 19 (22 Nov. 2019), p. 4878. issn: 14248220. doi: 10.3390/S19224878. url: /pmc/articles/PMC6891287/ /pmc/articles/PMC6891287/?report=abstracthttps://www.ncbi.nlm.nih.gov/pmc/articles/PMC6891287/.

[32] G. R. Müller-Putz, D. Zimmermann, B. Graimann, K. Nestinger, G. Korisek, and G. Pfurtscheller. "Event-related beta EEG-changes during passive and attempted foot movements in paraplegic patients." In: *Brain research* 1137 (1 Mar. 2007), pp. 84–91. issn: 0006-8993. doi: 10.1016/J.BRAINRES.2006.12.052. url: https://pubmed.ncbi.nlm.nih.gov/17229403/.

[33] E. López-Larraz, J. M. Antelis, L. Montesano, A. Gil-Agudo, and J. Minguez. "Continuous decoding of motor attempt and motor imagery from EEG activity in spinal cord injury patients." In: *2012 Annual International Conference of the IEEE Engineering in Medicine and Biology Society*. 2012, pp. 1798–1801. doi: 10.1109/EMBC.2012.6346299.

[34] Y. Blokland, L. Spyrou, D. Thijssen, T. Eijsvogels, W. Colier, M. Floor-Westerdijk, R. Vlek, J. Bruhn, and J. Farquhar. "Combined EEG-fNIRS Decoding of Motor Attempt and Imagery for Brain Switch Control: An Offline Study in Patients With Tetraplegia." In: *IEEE Transactions on Neural Systems and Rehabilitation Engineering* 22.2 (2014), pp. 222–229. doi: 10.1109/TNSRE.2013.2292995.

[35] S. Chen, X. Shu, H. Wang, L. Ding, J. Fu, and J. Jia. "The Differences Between Motor Attempt and Motor Imagery in Brain-Computer Interface Accuracy and Event-Related Desynchronization of Patients With Hemiplegia." In: *Frontiers in Neurorobotics* 15 (2021), p. 147. issn: 1662-5218. doi: 10.3389/fnbot.2021.706630. url: https://www.frontiersin.org/article/10.3389/fnbot.2021.706630.

[36] N. Padfield, J. Zabalza, H. Zhao, V. Masero, and J. Ren. "EEG-Based Brain-Computer Interfaces Using Motor-Imagery: Techniques and Challenges." In: (2019). doi: 10.3390/s19061423. url: www.mdpi.com/journal/sensors.

[37] Siuly. *ANALYSIS AND CLASSIFICATION OF EEG SIGNALS*. July 2012. url: https://eprints.usq.edu.au/23460/1/Siuly_2012_whole.pdf.

[38] A. Delval, M. Bayot, L. Defebvre, and K. Dujardin. "Cortical Oscillations during Gait: Wouldn't Walking be so Automatic?" In: *Brain sciences* 10 (2 Feb. 2020). issn: 2076-3425. doi: 10.3390/BRAINSCI10020090. url: https://pubmed.ncbi.nlm.nih.gov/32050471/.

[39] S. R. Sreeja, J. Rabha, D. Samanta, P. Mitra, and M. Sarma. "Classification of motor imagery based EEG signals using sparsity approach." In: *Lecture Notes in Computer Science (including subseries Lecture Notes in Artificial Intelligence and Lecture Notes in Bioinformatics)* 10688 LNCS (2017), pp. 47–59. issn: 16113349. doi: 10.1007/978-3-319-72038-8_5.

[40] *Motor Cortex (Section 3, Chapter 3) Neuroscience Online: An Electronic Textbook for the Neurosciences | Department of Neurobiology and Anatomy - The University of Texas Medical School at Houston*. url: https://nba.uth.tmc.edu/neuroscience/m/s3/chapter03.html.

[41] *The Anatomy of Movement - Brain Connection*. url: https://brainconnection.brainhq.com/2013/03/05/the-anatomy-of-movement/.

[42] "Brain-computer interfaces for post-stroke motor rehabilitation: a meta-analysis." In: *Annals of Clinical and Translational Neurology* 5 (5 2018), pp. 651–663. doi: 10.1002/acn3.544. url: https://www.ncbi..

[43] K. S. Mistry, P. Pelayo, D. G. Anil, and K. George. "An SSVEP based brain computer interface system to control electric wheelchairs." In: *2018 IEEE International Instrumentation and Measurement Technology Conference (I2MTC)*. 2018, pp. 1–6. doi: 10.1109/I2MTC.2018.8409632.

[44] F. Carrino, J. Dumoulin, E. Mugellini, O. A. Khaled, and R. Ingold. "A self-paced BCI system to control an electric wheelchair: Evaluation of a commercial, low-cost EEG device." In: *2012 ISSNIP Biosignals and Biorobotics Conference: Biosignals and Robotics for Better and Safer Living (BRC)*. 2012, pp. 1–6. doi: 10.1109/BRC.2012.6222185.

[45] A. Siswoyo, Z. Arief, and I. A. Sulistijono. "Application of Artificial Neural Networks in Modeling Direction Wheelchairs Using Neurosky Mindset Mobile (EEG) Device." In: *EMITTER International Journal of Engineering Technology* 5.1 (July 2017), pp. 170–191. doi: 10.24003/emitter.v5i1.165. url: https://emitter2.pens.ac.id/ojs/index.php/emitter/article/view/165.

[46] I. A. Mirza, A. Tripathy, S. Chopra, M. D'Sa, K. Rajagopalan, A. D'Souza, and N. Sharma. "Mind-controlled wheelchair using an EEG headset and arduino microcontroller." In: *2015 International Conference on Technologies for Sustainable Development (ICTSD)*. 2015, pp. 1–5. doi: 10.1109/ICTSD.2015.7095887.

[47] G. Schalk, D. McFarland, T. Hinterberger, N. Birbaumer, and J. Wolpaw. "BCI2000: a general-purpose brain-computer interface (BCI) system." In: *IEEE Transactions on Biomedical Engineering* 51.6 (2004), pp. 1034–1043. doi: 10.1109/TBME.2004.827072.

[48] M. A. A. Kasim, C. Y. Low, M. A. Ayub, N. A. C. Zakaria, M. H. M. Salleh, K. Johar, and H. Hamli. "User-Friendly LabVIEW GUI for Prosthetic Hand Control Using Emotiv EEG Headset." In: *Procedia Computer Science* 105 (2017). 2016 IEEE International Symposium on Robotics and Intelligent Sensors, IRIS 2016, 17-20 December 2016, Tokyo, Japan, pp. 276–281. issn: 1877-0509. doi: https://doi.org/10.1016/j.procs.2017.01.222. url: https://www.sciencedirect.com/science/article/pii/S1877050917302454.

[49] T. Beyrouthy, S. K. Al Kork, J. A. Korbane, and A. Abdulmonem. "EEG Mind controlled Smart Prosthetic Arm." In: *2016 IEEE International Conference on Emerging Technologies and Innovative Business Practices for the Transformation of Societies (EmergiTech)*. 2016, pp. 404–409. doi: 10.1109/EmergiTech.2016.7737375.

[50] R. Spicer, J. Anglin, D. M. Krum, and S.-L. Liew. "REINVENT: A low-cost, virtual reality brain-computer interface for severe stroke upper limb motor recovery." In: *2017 IEEE Virtual Reality (VR)*. 2017, pp. 385–386. doi: 10.1109/VR.2017.7892338.

[51] D. R. E. L. MD, A. N. S. MSc, H. Sandground, and M. B. DSc. "EEG-NeuroBioFeedback Treatment of Patients with Brain Injury: Part 2: Changes in EEG Parameters versus Rehabilitation." In: *Journal of Neurotherapy* 5.4 (2002), pp. 45–71. doi: 10.1300/J184v05n04_04. eprint: https://doi.org/10.1300/J184v05n04_04. url: https://doi.org/10.1300/J184v05n04_04.

[52] A. Shakeel, M. S. Navid, M. N. Anwar, S. Mazhar, M. Jochumsen, and I. K. Niazi. "A review of techniques for detection of movement intention using movement-related cortical potentials." In: *Computational and Mathematical Methods in Medicine* 2015 (2015). issn: 17486718. doi: 10.1155/2015/346217.

[53] J.-H. Jeong, N.-S. Kwak, M.-H. Lee, and S.-W. Lee. "Decoding of walking Intention under Lower limb exoskeleton Environment using MRCP Feature." In: *GBCIC*. 2017.

[54] L. F. Nicolas-Alonso and J. Gomez-Gil. "Brain Computer Interfaces, a Review." In: *Sensors* 12 (2012), pp. 1211–1279. issn: 1424-8220. doi: 10.3390/s120201211. url: www.mdpi.com/journal/sensors.

[55] A. Seeland, L. Manca, F. Kirchner, and E. A. Kirchner. "Spatio-temporal Comparison between ERD/ERS and MRCP-based Movement Prediction." In: (). doi: 10.5220/0005214002190226.

[56] E. López-Larraz, F. Trincado-Alonso, V. Rajasekaran, S. Pérez-Nombela, A. J. del Ama, J. Aranda, J. Minguez, A. Gil-Agudo, and L. Montesano. "Control of an Ambulatory Exoskeleton with a Brain-Machine Interface for Spinal Cord Injury Gait Rehabilitation." In: *Frontiers in neuroscience* 10 (AUG Aug. 2016). issn: 1662-4548. doi: 10.3389/FNINS.2016.00359. url: https://pubmed.ncbi.nlm.nih.gov/27536214/.

[57] Y. Li, X. Gao, H. Liu, and S. Gao. "Classification of single-trial electroencephalogram during finger movement." In: *IEEE transactions on bio-medical engineering* 51 (6 June 2004), pp. 1019–1025. issn: 0018-9294. doi: 10.1109/TBME.2004.826688. url: https://pubmed.ncbi.nlm.nih.gov/15188873/.

[58] Y. Wang, Z. Zhang, Y. Li, X. Gao, S. Gao, and F. Yang. "BCI Competition 2003-Data Set IV: An Algorithm Based on CSSD and FDA for Classifying Single-Trial EEG." In: *IEEE TRANSACTIONS ON BIOMEDICAL ENGINEERING* 51 (6 2004). doi: 10.1109/TBME.2004.826697.

[59] B. Wang and F. Wan. "Classification of single-trial EEG based on support vector clustering during finger movement." In: *Lecture Notes in Computer Science (including subseries Lecture Notes in Artificial Intelligence and Lecture Notes in Bioinformatics)* 5552 LNCS (PART 2 2009), pp. 354–363. issn: 16113349. doi: 10.1007/978-3-642-01510-6_41.

[60] R. Y. H. I. A. T. J; *Deep learning-based electroencephalography analysis: a systematic review*. url: https://pubmed.ncbi.nlm.nih.gov/31151119/.

[61] E. K. S. Louis. *Appendix 4. Common Artifacts During EEG Recording*. Jan. 1970. url: https://www.ncbi.nlm.nih.gov/books/NBK390358/.

[62] N. P. Subramaniyam. *Pitfalls of Filtering the EEG Signal - Sapien Labs: Neuroscience: Human Brain Diversity Project*. Nov. 2018. url: https://sapienlabs.org/pitfalls-of-filtering-the-eeg-signal/.

[63] W. A. E. B; *Digital filter design for electrophysiological data–a practical approach*. url: https://pubmed.ncbi.nlm.nih.gov/25128257/.

[64] A. Khatter, D. Bansal, and R. Mahajan. "Performance Analysis of IIR and FIR Windowing Techniques in Electroencephalography Signal Processing." In: *International Journal of Innovative Technology and Exploring Engineering* 8 (Sept. 2019). doi: 10.35940/ijitee.J9771.0881019.

[65] K. Veer, v. kumar, and S. Kumar. "Comparative study of FIR and IIR filters for the removal of 50 Hz noise from EEG signal." In: *International Journal of Medical Engineering and Informatics* 22 (Feb. 2016). doi: 10.1504/IJBET.2016.079488.

[66] D. J. McFarland, L. A. Miner, T. M. Vaughan, and J. R. Wolpaw. "Mu and Beta Rhythm Topographies During Motor Imagery and Actual Movements." In: *Brain Topography 2000 12:3* 12 (3 2000), pp. 177–186. issn: 1573-6792. doi: 10.1023/A:1023437823106. url: https://link.springer.com/article/10.1023/A:1023437823106.

[67] W. kin Tam, T. Wu, Q. Zhao, E. Keefer, and Z. Yang. "Human motor decoding from neural signals: a review." In: *BMC Biomedical Engineering 2019 1:1* 1 (1 Sept. 2019), pp. 1–22. issn: 2524-4426. doi: 10.1186/S42490-019-0022-Z. url: https://bmcbiomedeng.biomedcentral.com/articles/10.1186/s42490-019-0022-z.

[68] H. Yuan and B. He. "Brain–Computer Interfaces Using Sensorimotor Rhythms: Current State and Future Perspectives." In: *IEEE Transactions on Biomedical Engineering* 61.5 (2014), pp. 1425–1435. doi: 10.1109/TBME.2014.2312397.

[69] Z. Wang, C. Wang, G. Wu, Y. Luo, and X. Wu. *A control system of lower limb exoskeleton robots based on motor imagery*. 2017. doi: 10.1109/ICInfA.2017.8078925.

[70] F. Karimi, J. Kofman, N. Mrachacz-Kersting, D. Farina, and N. Jiang. "Detection of Movement Related Cortical Potentials from EEG Using Constrained ICA for Brain-Computer Interface Applications." In: *Frontiers in Neuroscience* 11 (JUN June 2017), p. 356. issn: 1662453X. doi: 10.3389/FNINS.2017.00356. url: /pmc/articles/PMC5492875//pmc/articles/PMC5492875/?report=abstracthttps://www.ncbi.nlm.nih.gov/pmc/articles/PMC5492875/.

[71] "Multiple kernel based region importance learning for neural classification of gait states from EEG signals." In: *Frontiers in Neuroscience* 11 (APR Apr. 2017), p. 170. issn: 1662453X. doi: 10.3389/FNINS.2017.00170/BIBTEX.

[72] A. Kilicarslan, S. Prasad, R. G. Grossman, and J. L. Contreras-Vidal. "High accuracy decoding of user intentions using EEG to control a lower-body exoskeleton." In: *2013 35th Annual International Conference of the IEEE Engineering in Medicine and Biology Society (EMBC)*. 2013, pp. 5606–5609. doi: 10.1109/EMBC.2013.6610821.

[73] "An integrated neuro-robotic interface for stroke rehabilitation using the NASA X1 powered lower limb exoskeleton." In: *Annual International Conference of the IEEE Engineering in Medicine and Biology Society. IEEE Engineering in Medicine and Biology Society. Annual International Conference, doi:10.1109/EMBC.2014.6944497,pmid:25570865* 2014 (Nov. 2014), pp. 3985–3988. issn: 2694-0604. doi: 10.1109/EMBC.2014.6944497. url: https://pubmed.ncbi.nlm.nih.gov/25570865/.

[74] A. R. Donati, S. Shokur, E. Morya, D. S. Campos, R. C. Moioli, C. M. Gitti, P. B. Augusto, S. Tripodi, C. G. Pires, G. A. Pereira, F. L. Brasil, S. Gallo, A. A. Lin, A. K. Takigami, M. A. Aratanha, S. Joshi, H. Bleuler, G. Cheng, A. Rudolph, and M. A. Nicolelis. "Long-Term Training with a Brain-Machine Interface-Based Gait Protocol Induces Partial Neurological Recovery in Paraplegic Patients." In: *Scientific reports* 6 (Aug. 2016). issn: 2045-2322. doi: 10.1038/SREP30383. url: https://pubmed.ncbi.nlm.nih.gov/27513629/.

[75] K. Lee, D. Liu, L. Perroud, R. Chavarriaga, and J. del R. Millán. "A brain-controlled exoskeleton with cascaded event-related desynchronization classifiers." In: *Robotics and Autonomous Systems* 90 (2017). Special Issue on New Research Frontiers for Intelligent Autonomous Systems, pp. 15–23. issn: 0921-8890. doi: https://doi.org/10.1016/j.robot.2016.10.005. url: https://www.sciencedirect.com/science/article/pii/S0921889016304948.

[76] A. Kilicarslan, R. G. Grossman, and J. L. Contreras-Vidal. "A robust adaptive denoising framework for real-time artifact removal in scalp EEG measurements." In: *Journal of Neural Engineering* 13 (2 Feb. 2016), p. 026013. issn: 1741-2552. doi: 10.1088/1741-2560/13/2/026013. url: https://iopscience.iop.org/article/10.1088/1741-2560/13/2/026013https://iopscience.iop.org/article/10.1088/1741-2560/13/2/026013/meta.

[77] L. Pion-Tonachini, S. H. Hsu, C. Y. Chang, T. P. Jung, and S. Makeig. "Online Automatic Artifact Rejection using the Real-time EEG Source-mapping Toolbox (REST)." In: *Proceedings of the Annual International Conference of the IEEE Engineering in Medicine and Biology Society, EMBS* 2018-July (Oct. 2018), pp. 106–109. issn: 1557170X. doi: 10.1109/EMBC.2018.8512191.

[78] C. Y. Chang, S. H. Hsu, L. Pion-Tonachini, and T. P. Jung. "Evaluation of Artifact Subspace Reconstruction for Automatic Artifact Components Removal in Multi-Channel EEG Recordings." In: *IEEE Transactions on Biomedical Engineering* 67 (4 Apr. 2020), pp. 1114–1121. issn: 15582531. doi: 10.1109/TBME.2019.2930186.

[79] D. J. McFarland, L. M. McCane, S. V. David, and J. R. Wolpaw. "Spatial filter selection for EEG-based communication." In: *Electroencephalography and Clinical Neurophysiology* 103.3 (1997), pp. 386–394. issn: 0013-4694. doi: https://doi.org/10.1016/S0013-4694(97)00022-2. url: https://www.sciencedirect.com/science/article/pii/S0013469497000222.

[80] *Feature Engineering for Machine Learning - Javatpoint*. url: https://www.javatpoint.com/feature-engineering-for-machine-learning.

[81] N. Brodu, F. Lotte, and A. Lécuyer. *Exploring two novel features for EEG-based brain–computer interfaces: Multifractal cumulants and predictive complexity*. Nov. 2011. url: https://www.sciencedirect.com/science/article/pii/S0925231211006291.

[82] *Performance analysis of LDA, QDA and KNN algorithms in left-right limb movement classification from EEG data*. url: https://ieeexplore.ieee.org/abstract/document/5735358/.

[83] D. O. G. G. EF; *Awareness and the EEG power spectrum: analysis of frequencies*. url: https://pubmed.ncbi.nlm.nih.gov/15377585/.

[84] F. Lotte, L. Bougrain, A. Cichocki, M. Clerc, M. Congedo, A. Rakotomamonjy, and F. Yger. "A review of classification algorithms for EEG-based brain-computer interfaces: A 10 year update." In: *Journal of Neural Engineering* 15 (3 Apr. 2018). issn: 17412552. doi: 10.1088/1741-2552/AAB2F2.

[85] "Single-trial analysis and classification of ERP components - A tutorial." English. In: *NeuroImage* 56.2 (May 2011), pp. 814–825. issn: 1053-8119. doi: 10.1016/j.neuroimage.2010.06.048.

[86] H. Ramoser, J. Muller-Gerking, and G. Pfurtscheller. "Optimal spatial filtering of single trial EEG during imagined hand movement." In: *IEEE Transactions on Rehabilitation Engineering* 8.4 (2000), pp. 441–446. doi: 10.1109/86.895946.

[87] K. Värbu. *Systematic Literature Review on EEG-based BCI Applications*. 2020. url: https://comserv.cs.ut.ee/home/files/EEGbasedBCIapplications(KaidoVarbu).pdf?study=ATILoputoo&reference=00F464117DCA1B1A421BC5E54CC773263DC843D2.

[88] D. Barahona, P. Karlsruhe, and A. Uk. "Chair for Embedded Systems Evaluation of Feature Extraction Techniques for an Internet of Things Electroencephalogram CORE View metadata, citation and similar papers at core." In: (2016).

[89] V. Jusas and S. G. Samuvel. "Classification of Motor Imagery Using Combination of Feature Extraction and Reduction Methods for Brain-Computer Interface." In: *Information Technology and Control* 48 (2 June 2019), pp. 225–234. issn: 2335-884X. doi: 10.5755/J01.ITC.48.2.23091. url: https://itc.ktu.lt/index.php/ITC/article/view/23091.

[90] G. Dornhege, B. Blankertz, G. Curio, and K.-R. Muller. "Boosting bit rates in noninvasive EEG single-trial classifications by feature combination and multiclass paradigms." In: *IEEE Transactions on Biomedical Engineering* 51.6 (2004), pp. 993–1002. doi: 10.1109/TBME.2004.827088.

[91] "What is Feature Selection? Definition and FAQs | OmniSci." In: (). url: https://www.omnisci.com/technical-glossary/feature-selection.

[92] B. Abbaszadeh, C. A. D. Teixeira, and M. C. Yagoub. "Feature Selection Techniques for the Analysis of Discriminative Features in Temporal and Frontal Lobe Epilepsy: A Comparative Study." In: *The Open Biomedical Engineering Journal* 15 (1 June 2021), pp. 1–15. issn: 1874-1207. doi: 10.2174/1874120702115010001.

[93] S. kaushik. "Feature Selection Methods | Machine Learning." In: (Dec. 2016). url: https://www.analyticsvidhya.com/blog/2016/12/introduction-to-feature-selection-methods-with-an-example-or-how-to-select-the-right-variables/.

[94] *Feature Selection Methods | Machine Learning*. url: https://www.analyticsvidhya.com/blog/2016/12/introduction-to-feature-selection-methods-with-an-example-or-how-to-select-the-right-variables/.

[95] A. Saibene and F. Gasparini. "GA for feature selection of EEG heterogeneous data." In: (Mar. 2021). url: http://arxiv.org/abs/2103.07117.

[96] S. V. Eslahi, J. Dabanloo, and K. Maghooli. "A GA-based feature selection of the EEG signals by classification evaluation: Application in BCI systems." In: ().

[97] C. Yaacoub, G. Mhanna, and S. Rihana. "A Genetic-Based Feature Selection Approach in the Identification of Left/Right Hand Motor Imagery for a Brain-Computer Interface." In: *Brain Sciences* 7 (2017).

[98] M. Z. Baig, N. Aslam, and H. P. Shum. "Filtering techniques for channel selection in motor imagery EEG applications: a survey." In: *Artificial Intelligence Review* 53 (2 Feb. 2020), pp. 1207–1232. issn: 15737462. doi: 10.1007/S10462-019-09694-8/TABLES/2. url: https://link.springer.com/article/10.1007/s10462-019-09694-8.

[99] Y. Wang, S. Cang, and H. Yu. "A survey on wearable sensor modality centred human activity recognition in health care." In: *Expert Systems with Applications* 137 (2019), pp. 167–190. issn: 0957-4174. doi: https://doi.org/10.1016/j.eswa.2019.04.057. url: https://www.sciencedirect.com/science/article/pii/S0957417419302878.

[100] *Supervised vs. Unsupervised Learning: What's the Difference?* url: https://www.ibm.com/cloud/blog/supervised-vs-unsupervised-learning.

[101] D. Delisle-Rodriguez, A. C. Villa-Parra, and T. Bastos. "Towards a Brain-Computer Interface Based on Unsupervised Methods to Command a Lower-Limb Robotic Exoskeleton." In: *2018 IEEE International Conference on Systems, Man, and Cybernetics (SMC)*. 2018, pp. 1099–1104. doi: 10.1109/SMC.2018.00194.

[102] A. Schlögl, F. Lee, H. Bischof, and G. Pfurtscheller. "Characterization of four-class motor imagery EEG data for the BCI-competition 2005." In: *Journal of Neural Engineering* 2 (4 Aug. 2005), p. L14. issn: 1741-2552. doi: 10.1088/1741-2560/2/4/L02. url: https://iopscience.iop.org/article/10.1088/1741-2560/2/4/L02https://iopscience.iop.org/article/10.1088/1741-2560/2/4/L02/meta.

[103] M. Saeidi, W. Karwowski, F. V. Farahani, K. Fiok, R. Taiar, P. A. Hancock, and A. Al-Juaid. "Neural Decoding of EEG Signals with Machine Learning: A Systematic Review." In: *Brain Sciences* 11.11 (2021). issn: 2076-3425. doi: 10.3390/brainsci11111525. url: https://www.mdpi.com/2076-3425/11/11/1525.

[104] S. Park, F. C. Park, J. Choi, and H. Kim. "EEG-based Gait State and Gait Intention Recognition Using Spatio-Spectral Convolutional Neural Network." In: *2019 7th International Winter Conference on Brain-Computer Interface (BCI)*. 2019, pp. 1–3. doi: 10.1109/IWW-BCI.2019.8737259.

[105] H. Dose, J. S. Møller, H. K. Iversen, and S. Puthusserypady. "An end-to-end deep learning approach to MI-EEG signal classification for BCIs." In: *Expert Systems with Applications* 114 (Dec. 2018), pp. 532–542. issn: 0957-4174. doi: 10.1016/J.ESWA.2018.08.031.

[106] S. Tortora, S. Ghidoni, C. Chisari, S. Micera, and F. Artoni. "Deep learning-based BCI for gait decoding from EEG with LSTM recurrent neural network." In: *Journal of Neural Engineering* 17.4 (July 2020), p. 046011. doi: 10.1088/1741-2552/ab9842. url: https://doi.org/10.1088/1741-2552/ab9842.

[107] F. Lotte, M. Congedo, A. Lécuyer, F. Lamarche, and B. Arnaldi. "A review of classification algorithms for EEG-based brain-computer interfaces." In: *Journal of neural engineering* 4 (2 June 2007). issn: 1741-2560. doi: 10.1088/1741-2560/4/2/R01. url: https://pubmed.ncbi.nlm.nih.gov/17409472/.

[108] D. AH, W. PT, K. CE, A. A, and N. Z. *Brain-computer interface controlled functional electrical stimulation system for ankle movement*. url: https://pubmed.ncbi.nlm.nih.gov/21867567/.

Appendix A

Appendix

		Study 1	Study 2	Study 3
CNN	Spectra	66.593% (+/- 7.458%)	76.875% (+/- 6.036%)	97.419% (+/- 2.414%)
	ERP	89.100% (+/- 2.267%)	98.300% (+/- 0.927%)	100.000% (+/- 0.000%)
	ERSP	92.682% (+/- 2.296%)	78.767% (+/- 3.661%)	69.912% (+/- 1.088%)
LSTM	Spectra	46.815% (+/- 3.498%)	65.423% (+/- 7.234%)	86.552% (+/- 3.698%)
	ERP	87.400% (+/- 1.960%)	98.900% (+/- 1.068%)	99.900% (+/- 0.200%)
	ERSP	91.763% (+/- 1.633%)	79.014% (+/- 2.174%)	73.056% (+/- 1.426%)
C-LSTM	Spectra	58.306% (+/- 4.755%)	81.472% (+/- 5.214%)	96.129% (+/- 4.741%)
	ERP	91.300% (+/- 2.421%)	99.500% (+/- 0.548%)	99.700% (+/- 0.400%)
	ERSP	93.822% (+/- 1.083%)	78.763% (+/- 1.975%)	75.325% (+/- 2.976%)

Table 9: Training Accuracy

		Study 1	Study 2	Study 3
CNN	Spectra	0.61	0.70	0.96
	ERP	0.90	0.97	1.00
	ERSP	0.90	0.77	0.66
LSTM	Spectra	0.29	0.61	0.84
	ERP	0.88	0.98	1.00
	ERSP	0.90	0.75	0.68
C-LSTM	Spectra	0.56	0.82	0.96
	ERP	0.94	0.98	0.99
	ERSP	0.94	0.72	0.73

Table 10: Training MCC

		Study 1	Study 2	Study 3
CNN	Spectra	68.69%	73.51%	96.77%
	ERP	91.94%	97.50%	100%
	ERSP	92.05%	81.74%	71.87%
LSTM	Spectra	45.15%	67.85%	87.00
	ERP	90.41%	98.49%	100%
	ERSP	92.31%	80.26%	74.23%
C-LSTM	Spectra	65.16%	81.42%	96.7%
	ERP	95.51%	98.48%	99.49%
	ERSP	94.67%	77.97%	78.19%

Table 11: Training F1 scores

	Study 1	Study 2	Study 3
CNN	86.40%	89.60%	96.00%
LSTM	85.60%	96.80%	95.60%
C-LSTM	89.60%	98.40%	99.60%

Table 12: Test Accuracy

	Study 1	Study 2	Study 3
CNN	0.83	0.87	0.94
LSTM	0.82	0.96	0.94
C-LSTM	0.87	0.98	0.99

Table 13: Test MCC

	Study 1	Study 2	Study 3
CNN	86.02%	89.37%	95.99%
LSTM	85.33%	96.80%	95.56%
C-LSTM	89.55%	98.40%	99.59%

Table 14: Test F1 scores